INCORPORATION OF MOIST PROCESSES AND A PBL PARAMETERIZATION INTO THE GENERALIZED VERTICAL COORDINATE MODEL

by

Celal S. Konor
Department of Atmospheric Science, Colorado State University, Colorado,

Akio Arakawa
Department of Atmospheric and Oceanic Sciences, UCLA, California

Research supported by
the U. S. DOE under Grant number DE-FG02-04ER63848 and DE-FG02-02ER63370
to Colorado State University
and CSU Contract G-3816-3 to UCLA
and NOAA under Grant number NA030 AR4310095 to UCLA
and NFS under Grant number ATM-0415184 to Colorado State University

Department of Atmospheric Science
Colorado State University
Fort Collins, Colorado

December 2005

Atmospheric Science Paper No. 765

Incorporation of Moist Processes and a PBL Parameterization into the Generalized Vertical Coordinate Model

Celal S. Konor
Department of Atmospheric Science, Colorado State University

and

Akio Arakawa
Department of Atmospheric and Oceanic Sciences, UCLA

FOREWORD

This technical report presents a detailed description of the large-scale condensation process and PBL parameterization incorporated into the generalized coordinate model originally developed by Konor and Arakawa (1997).

The incorporation procedure for the large-scale condensation closely follows Konor and Arakawa (2000) since the generalized vertical coordinate is virtually an isentropic coordinate for a large part of the vertical domain.

The PBL parameterization presented here is an extension of that used in the UCLA-GCM, which is based on a single mixed layer with variable depth (Randall, 1976 and Suarez et al., 1983). Our version uses multiple layers while approximately maintaining the advantages of the original parameterization. In this parameterization, the bulk formulation is used for the effects of convectively active large eddies and a newly introduced K-closure formulation is used for the effects of diffusive small eddies. The bulk formulation, which is originally introduced by Randall, Branson, Zhang, Moeng and Krasner (unpublished, partially based on Krasner, 1993), is based on a predicted bulk turbulence kinetic energy and explicitly determined PBL-top entrainment. The entrainment formulation is discussed by Randall and Schubert (2004).

Corresponding author address: Dr. Celal S. Konor, Department of Atmospheric Science, Colorado State University, Fort Collins, CO 80523-1371. *E-mail:* csk@atmos.ucla.edu or csk@atmos.colostate.edu

Table of Contents

1-Introduction

An advantage of using a hybrid vertical coordinate, which combines an isentropic coordinate with a sigma-type coordinate near the Earth's surface with a smooth transition between them, is well recognized. Detailed discussions on this topic can be found in Bleck and Benjamin (1993) and Konor and Arakawa (1997). Here we focus on the incorporation of condensation and PBL processes into our generalized vertical coordinate model, which is primarily designed to operate with an isentropic-sigma hybrid vertical coordinate (Konor and Arakawa, 1997). The incorporation of condensation process closely follows Konor and Arakawa (2000) since the hybrid coordinate we consider here is closed to an isentropic coordinate for a large part of the model's vertical domain.

In an isentropic coordinate, the vertical mass redistribution is solely through heating while the horizontal mass distribution is through horizontal advection along an isentropic surface. It is then easier to keep track of the budgets of prognostic variables in a discrete system with an isentropic coordinate than in that with a pressure-based coordinate. It should be noted, however, the way in which heating can be incorporated into a model with an isentropic coordinate is different from that into a model with a pressure-based coordinate. This is because the pressure distribution on the isentropic surfaces determines the thermal structure in an isentropic coordinate model while, in a pressure coordinate model, the potential temperature distribution determines the thermal structure as discussed by Konor and Arakawa (2000) in detail.

It has been widely recognized that the planetary boundary layer (PBL) plays a crucial role in the climate system. The representation of PBL processes, however, remains one of the major unresolved issues in climate modeling due to the complexity of the physical processes involved. The situation is especially serious for the PBL with a stratocumulus cloud layer inside.

The scale of turbulence in the PBL can be classified into two categories: the quasi-local small eddies and the non-local large eddies. This has led to two separate approaches in the formulation of PBL processes in atmospheric models: one emphasizes the small eddies by parameterizing their effects through a K-closure formulation (Louis, 1979) and the other emphasizes the large eddies by parameterizing their effects through a bulk approach, which implicitly includes the diffusive effects by assuming a well-mixed

PBL (Lilly, 1968). In later years, the K-closure formulation has been extended to include non-local effects by skewing the K-profile and including a countergradient flux term (Holtzlag and Moeng, 1991; Holtslag and Boville, 1993).

The behavior and structure of the clear convective PBL is relatively well understood and, therefore, its realistic simulation is the starting point of any comprehensive PBL parameterization. It is widely accepted that the two approaches mentioned above perform reasonably well in simulating major aspects of clear PBL. If the PBL top is higher than the condensation level, however, a cloudy sublayer forms within the PBL near the top. In this sublayer, turbulence is primarily driven by the convection due to the radiative cooling near the cloud top. Therefore, the cloud-topped PBL can be maintained even without positive buoyancy due to a surface heat flux. The mixed-layer approach comprises a straightforward formulation of turbulence fluxes in such a PBL (Lilly, 1968) while the K-closure approach does not.

A PBL parameterization based on the mixed-layer approach complemented by Deardorff's (1972) bulk parameterization for the variable-depth PBL is incorporated into the UCLA GCM (Randall 1976, Suarez et al. 1983). In this model, the layer next to the lower boundary is designated as the PBL, which acts as a well-mixed layer (see Fig. 1a). The parameterized mass entrainment (detrainment) into (out of) the PBL at the PBL top contributes to the rate of change of the PBL depth. The PBL temperature, moisture and wind fields are predicted using the parameterized surface fluxes and the fluxes associated with the entrainment (or detrainment) through the PBL top.

The use of a variable-depth well-mixed PBL greatly simplifies parameterization of PBL cloud processes. In particular, formulation of physical processes concentrated near the cloud top is much more tractable with this approach. The successful simulation of time-averaged stratocumulus cloud incidence with a recent version of the UCLA GCM (Li et al. 1999) is largely due to this advantage. The approach has disadvantages, however, some of which are listed below. First, it does not allow the vertical variation of the horizontal velocity within the PBL. Vertical resolution required for representing low-level baroclinicity, therefore, may be lost, especially when the PBL is deep. Moreover, even conservative thermodynamic variables, such as the moist static energy and the total water mixing ratio, which are assumed to be well-mixed in the bulk approach, are not always well-mixed in reality, especially for the stable PBL. Secondly, an inevitable large

jump in the vertical resolution between the PBL and the layer above in high vertical resolution models can cause large truncation errors.

The majority of climate models do not explicitly treat the PBL clouds. Among the ones with explicit treatment, for example, Gordon and Stern (1982) and Sud and Walker (1992) use an empirical formulation based on relative humidity; Hansen et al. (1983) uses a prognostic cloud water formulation; and Suarez et al. (1983), Randall et al. (1989) and the model we present here use the mixed-layer approach for the treatment of PBL clouds. A comprehensive review about the performance of the PBL cloud treatments can be found in Wyngaard and Moeng (1990). More recently, Lock et al. (2000) developed a formulation in which the treatment is based on an extended empirical relative humidity formulation. Lock's scheme is now used in the UKMO and GFDL models.

In recent years, there are efforts to incorporate the variable-depth PBL approach in the models based on the local and non-local K-formulations to improve the simulation of PBL cloud incident (Beljaars and Viterbo, 1998; Lock et al., 2000; Grenier and Bretherton, 2001). In these applications, the PBL is not an explicit model layer such as the one discussed in previous two paragraphs, but the PBL depth is diagnosed or predicted, locating the PBL-top anywhere between the levels of the model that are more or less fixed in space. Then, the PBL-top jump is generally obtained through an extrapolation technique from above and below. In this approach, therefore, the difficulty in maintaining a physically consistent PBL-top jump remains as a major problem.

An interesting approach gaining momentum is the mass-flux concept based on a convective circulation model (see Arakawa 1969, Arakawa 2000). The concept has been applied to the PBL parameterization problem for more than three decades by several authors. Most recent examples are Lappen and Randall (2001a,b,c), Bretherton et al. (2004), and McCaa and Bretherton (2004). The mass-flux concept appears to be useful in parameterizing the horizontal structure of the PBL, especially in determining the horizontal cloud distribution in transition from stratus to stratocumulus regimes. We recognize this approach as complimentary to the parameterization we discuss in this here.

In this technical note, we propose a hybrid approach that introduces multiple model layers within the PBL to resolve its internal structure, while retaining the advantages of the bulk parameterization (see Fig. 1b). In this approach, the bulk

formulation is used for the effects of convectively active large eddies, and a K-closure formulation is used for the effects of diffusive small eddies as in Randall (1976). Simulated profiles in the PBL are allowed to deviate from well-mixed profiles. The deviations are, however, assumed to be small for thermodynamic conservative variables in formulating bulk properties of the PBL.

We implemented this approach in vertically discrete models, using a vertical coordinate system in which the PBL-top is a coordinate surface shared by both the free atmosphere and the PBL. In this way, as we mentioned earlier, the formulation of the processes that are highly concentrated near the PBL top becomes more explicit. When the PBL does not have a well-defined top, such as the left-over "daytime" PBL in evening, the definition of this coordinate system becomes ambiguous. In such a situation, the coordinate can be viewed as an arbitrarily chosen coordinate.

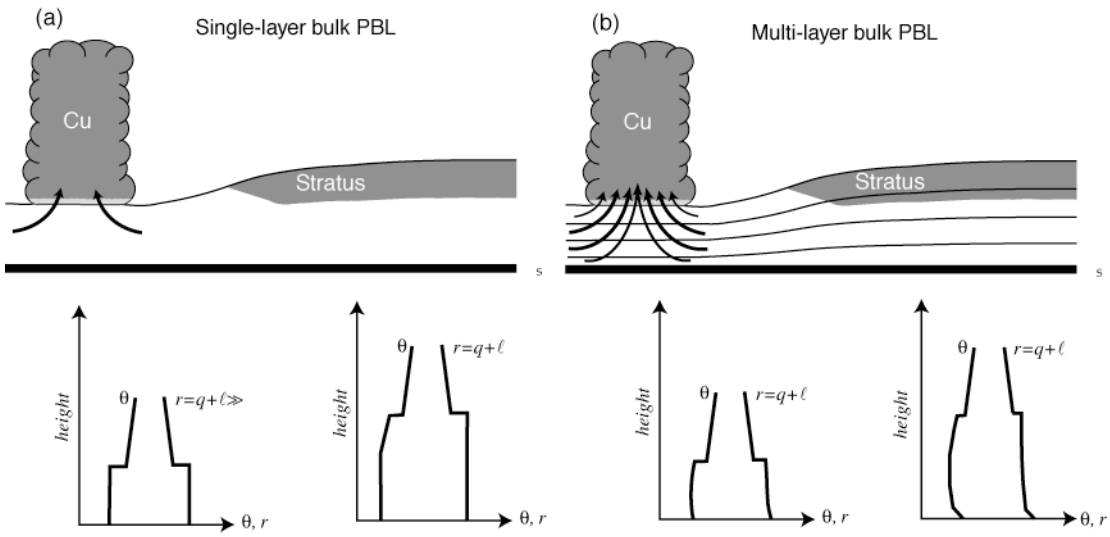

Fig. 1. Schematic representation of parameterized PBL a) based on a single layer as in current UCLA GCM and b) based on the multi-layers. Lower panel illustrates typical vertical profiles of the potential temperature θ and the total water mixing ratio r.

A major advantage of such a hybrid parameterization is in the simulation of the PBL processes during the surface frontogenesis. The multi-layer formulation allows vertical wind shears to be developed and maintained within the PBL due to the vertically varying pressure gradient force, while the potential temperature is nearly well mixed in the vertical. In this way, we may expect more realistic simulations of

extratropical cyclones and better prediction of low-level cloud distributions in the middle latitudes with this parameterization.

The PBL-top entrainment (or detrainment), PBL cloud processes and the surface fluxes are formulated following a new approach based on the predicted bulk turbulence kinetic energy (TKE), originally introduced by Randall, Branson, Zhang, Moeng and Krasner (personal communications; hereafter, RBZMK). The most important aspects of this approach can be found in Krasner (1993), Zhang et al. (1996), Randall et al., (1998) and Randall and Schubert (2004). The bulk properties of the PBL to be used in our formulations are obtained by mass-weighted vertical averaging of the prognostic variables over the entire PBL. In the case of potential temperature, averaging is only over the sub-cloud layers.

Motivated with the encouraging results obtained from this model, we incorporated the multi-layer PBL parameterization into the UCLA GCM. The results obtained by selected climate simulations will be presented in a forthcoming paper .

In the next section, we discuss the vertical coordinate for the free-atmosphere/PBL system. The basic governing equations are presented in section 3. The incorporation of condensation process into continuous system for the free atmosphere is discussed in section 4. We discuss the vertical discretization of the equations for the free atmosphere and PBL in section 5. The discretization of the PBL processes and the bulk PBL parameterization, which represents the effects of large convective eddies, are discussed in section 6 and 7, respectively. In section 8, we discuss the K-closure formulation representing the effects of the small diffusive eddies. In section 9, the free-atmosphere/PBL exchange processes are discussed. The additional discretization aspects of the model are presented in section 10. In section 11, we present a numerical simulation of extratropical cyclone evolution. Finally, a summary is presented in section 12.

2- Vertical coordinate

We have incorporated a multi-layer PBL parameterization with variable PBL depth into the generalized vertical coordinate model (see Fig. 2). A "massless" layer bounded by B^+ and B^- surfaces are added to the PBL top to represent the discontinuity in the predicted quantities between the free atmosphere and the PBL. When it is necessary, we will denote B^+ or B^- otherwise B will denote the PBL-top. Note that $\zeta_B = \zeta_{B^+} = \zeta_{B^-}$ and $p_B = p_{B^+} = p_{B^-}$ but, for example, $\theta_{B^+} \neq \theta_{B^-}$. To include the parameterized PBL, we define the vertical coordinate as

$$\zeta \equiv \begin{cases} F(\theta,\sigma) & \text{for } p_B \geq p \geq p_T \\ F^*(\sigma^*) & \text{for } p_S \geq p \geq p_B \end{cases}, \tag{2.1}$$

where p_S, p_B and p_T are the pressures at the surface, PBL-top and the top of the model atmosphere, respectively, and $\sigma \equiv (p_B - p)(p_B - p_T)^{-1}$ and $\sigma^* \equiv (p_S - p)(p_S - p_B)^{-1}$. (Note that, unlike the conventional sigma, our σ and σ^* increase in height.)

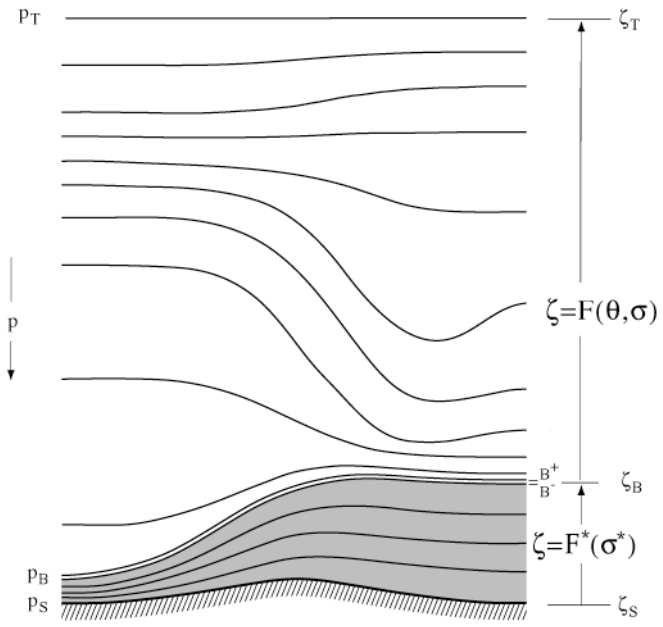

Fig. 2. The vertical structure of the model. The shaded area represents the PBL.

In the free atmosphere, where $p \le p_B$, the vertical coordinate is a hybrid θ-σ coordinate used by Konor and Arakawa (1997), which can be briefly described as follows: $F(\theta,\sigma) \equiv f(\sigma) + \theta g(\sigma)$, where $g(\sigma)$ is monotonic function of σ satisfying $g(\sigma) = 0$ at $\sigma = \sigma_B$ (=0) and $g(\sigma) = 1$ at $\sigma = \sigma_T$ (=1). To maintain ζ as a monotonic function of σ, it is required that $df/d\sigma = -\theta_{min}\, dg/d\sigma - (\partial\theta/\partial\sigma)_{min}\, g$, where θ_{min} and $(\partial\theta/\partial\sigma)_{min}$ are properly chosen lower bounds of θ and $d\theta/d\sigma$, respectively. Following Konor and Arakawa (1997), we use $g(\sigma) \equiv (1 - e^{-a\sigma})(1 - e^{-a})^{-1}$, where a is a constant. (We currently use a=10.)

In the PBL, we use a σ-type coordinate defined by $F^*(\sigma^*) \equiv \zeta_B + (\zeta_S - \zeta_B)(\sigma^* - \sigma_B^*)(\sigma_S^* - \sigma_B^*)^{-1}$, where $\sigma_S^* \equiv 0$, $\sigma_B^* \equiv 1$, $\zeta_B \equiv f(0)$ and $\zeta_S = \gamma\,\zeta_B$, where γ is an arbitrarily prescribed constant less than 1.

3- Basic governing equations

Here we present the basic governing equations including moist processes for the generalized vertical coordinate system. The mass continuity equation is given by

$$\left(\frac{\partial}{\partial t}\right)_\zeta m + \nabla_\zeta \cdot (m\mathbf{v}) + \frac{\partial}{\partial\zeta}(m\dot{\zeta}) = 0 \quad \text{for } \zeta_T > \zeta > \zeta_S, \qquad (3.1)$$

where

$$m \equiv -\partial p/\partial\zeta \ (>0). \qquad (3.2)$$

$(m\dot{\zeta})$ is the vertical mass flux, and $\dot{\zeta} \equiv D\zeta/Dt$ is the "vertical velocity". The material time-derivative is given by $D/Dt \equiv (\partial/\partial t)_\zeta + \mathbf{v}\cdot\nabla_\zeta + \dot{\zeta}\,\partial/\partial\zeta$. The pressure tendency equations can be obtained by vertically integrating (3.1) and (3.2) as

$$\left.\begin{aligned}
&\left(\frac{\partial}{\partial t}\right)_\zeta p = -\int_\zeta^{\zeta_T} \nabla_\zeta \cdot (m\mathbf{v})\,d\zeta + \left(m\dot{\zeta}\right) && \text{for } \zeta_T > \zeta > \zeta_B \qquad (3.3a)\\
&\left(\frac{\partial}{\partial t}\right)_\zeta p_B = -\int_{\zeta_B}^{\zeta_T} \nabla_\zeta \cdot (m\mathbf{v})\,d\zeta + \left(m\dot{\zeta}\right)_B && \text{for } \zeta = \zeta_B \qquad (3.3b)\\
&\left(\frac{\partial}{\partial t}\right)_\zeta p = \left(\frac{\partial}{\partial t}\right)_\zeta p_B - \int_\zeta^{\zeta_B} \nabla_\zeta \cdot (m\mathbf{v})\,d\zeta + \left(m\dot{\zeta}\right) - \left(m\dot{\zeta}\right)_B && \text{for } \zeta_B > \zeta > \zeta_S \qquad (3.3c)\\
&\left(\frac{\partial}{\partial t}\right)_\zeta p_S = \left(\frac{\partial}{\partial t}\right)_\zeta p_B - \int_{\zeta_S}^{\zeta_B} \nabla_\zeta \cdot (m\mathbf{v})\,d\zeta - \left(m\dot{\zeta}\right)_B && \text{for } \zeta = \zeta_S \qquad (3.3d)
\end{aligned}\right\},$$

where we assumed $\left(\partial p_T/\partial t\right)_\zeta = 0$. In (3.3a) to (3.3c), the vertical mass flux $\left(m\dot{\zeta}\right)$ for $\zeta_T > \zeta > \zeta_B$ is yet to be determined and the PBL-top mass flux $\left(m\dot{\zeta}\right)_B$ will be determined by physical parameterizations.

The thermodynamic equations used in the model are

$$\left.\begin{aligned}
&\left(\frac{\partial}{\partial t}\right)_\zeta \theta + \mathbf{v}\cdot\nabla_\zeta\theta + \frac{\partial\theta}{\partial\zeta}\dot{\zeta} = \frac{Q}{\Pi} && \zeta_T \ge \zeta \ge \zeta_{B^+} \quad (3.4a)\\
&\left(\frac{\partial}{\partial t}\right)_\zeta (m\theta) + \nabla_\zeta\cdot(m\theta\mathbf{v}) + \frac{\partial}{\partial\zeta}\left(\theta m\dot{\zeta}\right) = m\frac{Q}{\Pi} - g\frac{\partial F_\theta}{\partial\zeta} + G_\theta && \zeta_{B^-} > \zeta \ge \zeta_S \quad (3.4b)
\end{aligned}\right\},$$

where $\Pi \equiv c_p\left(p/p_o\right)^\kappa$ is the Exner function, Q is diabatic heating rate per unit mass, F_θ is the convective eddy fluxes of the potential temperature and G_θ is the additional effects in the PBL such as those due to diffusive eddy flux and cumulus roots. In the free atmosphere, we use the advective form (3.4a) to predict the potential temperature to automatically satisfy $\left(\partial\theta/\partial t\right)_\zeta = 0$ when $\zeta = \theta$. When we only consider condensation process, the heating rate Q is given by

$$Q = LC, \qquad (3.5)$$

where L is the latent heat and C is the condensation rate.

At present, liquid water is carried as a prognostic variable only within the PBL. For this case, the moisture budget equations are given by

$$\left.\begin{aligned}
&\left(\frac{\partial}{\partial t}\right)_\zeta (m q) + \nabla_\zeta \cdot (q m \mathbf{v}) + \frac{\partial}{\partial \zeta}\left(q m \dot{\zeta}\right) = -m C \qquad \zeta_T \ge \zeta \ge \zeta_{B^+} \qquad (3.6a)\\
&\left(\frac{\partial}{\partial t}\right)_\zeta (m r) + \nabla_\zeta \cdot (r m \mathbf{v}) + \frac{\partial}{\partial \zeta}\left(r m \dot{\zeta}\right) = -m \mathcal{R} - g \frac{\partial F_r}{\partial \zeta} + G_r \qquad \zeta_{B^-} > \zeta \ge \zeta_S \qquad (3.6b)
\end{aligned}\right\},$$

where q and r are the mixing ratios of water vapor and total water, respectively. The liquid water-mixing ratio is then given by $\ell = r - q^*$ if $r > q^*$ and $\ell = 0$ if $r \le q^*$, where q^* is the water vapor saturation mixing ratio. In (3.6b), $\mathcal{R}$ is the rate of raindrop generation, F_r is the convective eddy fluxes of the moisture. G_r represents additional effects in the PBL such as those due to diffusive eddy flux and cumulus roots.

The momentum equations used in the model are

$$\left.\begin{aligned}
&\left(\frac{\partial}{\partial t}\right)_\zeta \mathbf{v} + \mathbf{v}\cdot\nabla_\zeta \mathbf{v} + \frac{\partial \mathbf{v}}{\partial \zeta}\dot{\zeta} = -\left(\nabla_p \Phi\right) - f\,\mathbf{k}\times\mathbf{v} \qquad \zeta_T \ge \zeta \ge \zeta_{B^+} \quad (3.7a)\\
&\left(\frac{\partial}{\partial t}\right)_\zeta \mathbf{v} + \mathbf{v}\cdot\nabla_\zeta \mathbf{v} + \frac{\partial \mathbf{v}}{\partial \zeta}\dot{\zeta} = -\left(\nabla_p \Phi\right) - f\,\mathbf{k}\times\mathbf{v} - \frac{g}{m}\frac{\partial \mathbf{F_v}}{\partial \zeta} + \frac{\mathbf{G_v}}{m} \qquad \zeta_{B^-} > \zeta \ge \zeta_S \quad (3.7b)
\end{aligned}\right\},$$

where $-\left(\nabla_p \Phi\right)$ is the horizontal pressure gradient force, $\mathbf{F_v}$ is the convective eddy fluxes of the momentum. $\mathbf{G_v}$ represents additional effects in the PBL such as those due to diffusive eddy flux and cumulus roots. With the ζ coordinate, the horizontal pressure gradient force can be expressed as

$$-\nabla_p \Phi = -\nabla_\zeta M + \Pi \nabla_\zeta \theta\,, \qquad (3.8)$$

where M $(\equiv \Pi\theta + \Phi)$ is the Montgomery potential.

The hydrostatic equation used in the model is

$$\frac{\partial \Phi}{\partial \zeta} = m\left(\frac{\partial \Pi}{\partial p}\right)\theta_v\,, \qquad (3.9)$$

where θ_v is the virtual potential temperature defined by

$$\theta_v \equiv \theta\left(1 + 0.608\,q - \ell\right). \tag{3.10}$$

The hydrostatic equation (3.9) is used to determine the geopotential height Φ.

In the hybrid coordinate $\zeta = F(\theta,\sigma)$, ζ remains unchanged on each coordinate surface. We therefore require that

$$0 = \left(\frac{\partial}{\partial t}\right)_\zeta F(\theta,\sigma) \text{ for } \zeta_T \geq \zeta \geq \zeta_B. \tag{3.11}$$

From (3.11) we can derive a diagnostic relationship that determines the vertical mass flux $\left(m\dot{\zeta}\right)$. To do this, first expressing the right hand side of (3.11) as

$$\left(\frac{\partial F}{\partial \theta}\right)_\sigma \left(\frac{\partial \theta}{\partial t}\right)_\zeta + \left(\frac{\partial F}{\partial \sigma}\right)_\theta \left[\left(\frac{\partial \sigma}{\partial p_B}\right)_p \left(\frac{\partial p_B}{\partial t}\right) + \left(\frac{\partial \sigma}{\partial p}\right)_{p_B} \left(\frac{\partial p}{\partial t}\right)_\zeta\right] = 0 \tag{3.12}$$

and then using (3.3a) and (3.3b), we obtain

$$\left[\left(\frac{\partial F}{\partial \theta}\right)_\sigma \frac{1}{m}\frac{\partial \theta}{\partial \zeta} - \left(\frac{\partial F}{\partial \sigma}\right)_\theta \left(\frac{\partial \sigma}{\partial p}\right)_{p_B}\right]\left(m\dot{\zeta}\right) = \left(\frac{\partial F}{\partial \theta}\right)_\sigma \left(\frac{Q}{\Pi} - \mathbf{v}\cdot\nabla_\zeta \theta\right) +$$

$$\left(\frac{\partial F}{\partial \sigma}\right)_\theta \left\{\left(\frac{\partial \sigma}{\partial p_B}\right)_p \left[-\int_{\zeta_B}^{\zeta_T} \nabla_\zeta \cdot (m\mathbf{v})\,d\zeta + \left(m\dot{\zeta}\right)_B\right] + \left(\frac{\partial \sigma}{\partial p}\right)_{p_B} \left[-\int_\zeta^{\zeta_T} \nabla_\zeta \cdot (m\mathbf{v})\,d\zeta\right]\right\}. \tag{3.13}$$

Here we have used $\left(\partial p_T/\partial t\right) = 0$. Equation (3.13) is a generalized vertical mass flux equation. When $F \equiv \sigma$, $\left(m\dot{\sigma}\right)_B = 0$ and $\dot{\zeta} \equiv \dot{\sigma}$, (3.13) yields

$$\left(m\dot{\sigma}\right) = \nabla_\sigma \cdot \int_\sigma^{\sigma_T} (m\mathbf{v})\,d\sigma - (1-\sigma)\nabla_\sigma \cdot \int_{\sigma_B}^{\sigma_T} (m\mathbf{v})\,d\sigma, \tag{3.14}$$

which is equivalent to the vertical mass flux equation for a σ coordinate. (Note that, in our definition of the vertical coordinate, σ increases with height.) On the other hand,

when $F \equiv \theta$ and $\dot{\zeta} \equiv \dot{\theta}$, (3.13) yields

$$\dot{\theta} = \frac{Q}{\Pi}, \tag{3.15}$$

which is the vertical mass flux for the isentropic coordinate.

Within the PBL ζ also remains unchanged on each coordinate surface. We therefore require that

$$0 = \left(\frac{\partial}{\partial t}\right)_{\zeta} F^{*}\left(\sigma^{*}\right) \text{for} \zeta_{B} \geq \zeta \geq \zeta_{S}. \tag{3.16}$$

From (3.16), we can derive a diagnostic relationship that determines the vertical mass flux $\left(m\dot{\zeta}\right)$ within the PBL. To do this, we first express the right hand side of (3.16) as

$$\left(\frac{\partial \sigma^{*}}{\partial p_{B}}\right)_{p,p_{S}} \left(\frac{\partial p_{B}}{\partial t}\right)_{\zeta} + \left(\frac{\partial \sigma^{*}}{\partial p}\right)_{p_{B},p_{S}} \left(\frac{\partial p}{\partial t}\right)_{\zeta} + \left(\frac{\partial \sigma^{*}}{\partial p_{S}}\right)_{p,p_{B}} \left(\frac{\partial p_{S}}{\partial t}\right)_{\zeta} = 0 \text{ for} \zeta_{B} \geq \zeta \geq \zeta_{S}. \tag{3.17}$$

Then using (3.3b) to (3.3d) in (3.17), we obtain the equation that determines the vertical mass flux within the PBL as

$$\left(m\dot{\zeta}\right) = \sigma^{*}\left(m\dot{\zeta}\right)_{B} + \int_{\zeta}^{\zeta_{B}} \nabla_{\zeta} \cdot \left(m\mathbf{v}\right) d\zeta - \left(1-\sigma^{*}\right) \int_{\zeta_{S}}^{\zeta_{B}} \nabla_{\zeta} \cdot \left(m\mathbf{v}\right) d\zeta \text{ for} \zeta_{B} \geq \zeta \geq \zeta_{S}. \tag{3.18}$$

Note that we can also write $\sigma^{*} = \left(\zeta_{S} - \zeta\right)\left(\zeta_{S} - \zeta_{B}\right)^{-1}$ within the PBL.

4-Formulation of large-scale condensation within the free atmosphere

As in (3.11), we are requiring

$$\left(\frac{\partial}{\partial t}\right)_{\zeta} F\left(\theta, \sigma\right) = 0 \quad \text{for} \quad \zeta_{T} \geq \zeta \geq \zeta_{B} \tag{4.1}$$

in the free atmosphere. Now let us consider the large-scale condensation process, in which condensation heating at a given ζ changes θ and p locally while p_B is not directly effected. Then, from (4.1), we can write

$$\left(\frac{\partial F}{\partial \theta}\right)_\sigma \left(\frac{\partial \theta}{\partial t}\right)_\zeta + \left(\frac{\partial F}{\partial \sigma}\right)_\theta \left(\frac{\partial \sigma}{\partial p}\right)_{p_B} \left(\frac{\partial p}{\partial t}\right)_\zeta = 0 . \tag{4.2}$$

When only the direct effects of condensation process are considered, (3.4a) and (3.3a) give

$$\left.\begin{aligned} \left(\frac{\partial}{\partial t}\right)_\zeta \theta &= \frac{Q}{\Pi} - \frac{\partial \theta}{\partial \zeta}\dot{\zeta} \\ \left(\frac{\partial}{\partial t}\right)_\zeta p &= m\dot{\zeta} \end{aligned}\right\} . \tag{4.3}$$

We can then obtain an equation that determines the "vertical velocity" induced by condensation heating by eliminating the terms with time derivatives between (4.3) and (4.2) as

$$\dot{\zeta} = A\frac{Q}{\Pi}, \tag{4.4}$$

where A is defined by

$$A \equiv \frac{\left(\partial F/\partial \theta\right)_\sigma}{\left(\partial F/\partial \theta\right)_\sigma \left(\partial \theta/\partial \zeta\right) - m\left(\partial F/\partial \sigma\right)_\theta \left(\partial \sigma/\partial p\right)_{p_B}} . \tag{4.5}$$

A is a parameter between 0 and 1 that relates $\dot{\zeta}$ to heating Q. For an isentropic coordinate, $F \equiv \theta$, equation (4.5) yields A=1 since $\left(\partial F/\partial \theta\right)_\sigma = 1$ and $\left(\partial F/\partial \sigma\right)_\theta = 0$. The "vertical velocity" then becomes $\dot{\zeta} \equiv \dot{\theta} = Q/\Pi$ implying that the heating and the vertical mass flux are directly related. (For more detail see Konor and Arakawa, 2000.) For $F \equiv \sigma$, on the other hand, since yields $A = 0$ since $\left(\partial F/\partial \theta\right)_\sigma = 0$ and $\left(\partial F/\partial \sigma\right)_\theta = 1$. Then $\dot{\zeta} = 0$ so that the vertical mass flux is not directly related to the heating in the sense

that only the mass continuity equation determines the vertical mass flux.

The change in the water vapor mixing ratio *due to condensation* is determined by

$$\left(\frac{\partial}{\partial t}\right)_{\zeta} q = -C - A\frac{Q}{\Pi}\left(\frac{\partial q}{\partial \zeta}\right). \tag{4.6}$$

For a saturated atmosphere, $q = q^{*}(\theta, p)$, water vapor mixing ratio is controlled by potential temperature and pressure. When the advection terms are restored in (4.6), the rate of condensation depends upon the vertical mass flux. Then the primary effect of condensation heating due to saturation on the flow is to modify, often to reduce depending upon the lapse-rate, the effective static stability of the atmosphere. This issue for an isentropic coordinate is discussed by Konor and Arakawa (2000) in detail.

5- Vertical grid and discretization of equations

5.a. Vertical grid

The atmosphere is divided into L+M layers identified by integer indices and L+M+1 interfaces of the layers identified by half-integer indices (see Fig. 3). These indices increase downward (while ζ increases upward). The free atmosphere occupies L layers from the top of the model atmosphere, which is the upper most coordinate surface identified by T or 1/2, to the PBL top, which is also a coordinate surface identified by B or L+1/2. The PBL is divided into M layers from the PBL-top to the surface, which is identified by S or M+1/2. In the free atmosphere, horizontal velocity **v** and mass m are predicted for the model layers, while the potential temperature θ and the water vapor mixing ratio q are predicted for the interfaces of the layers where vertical velocity $\dot{\zeta}$ is carried.

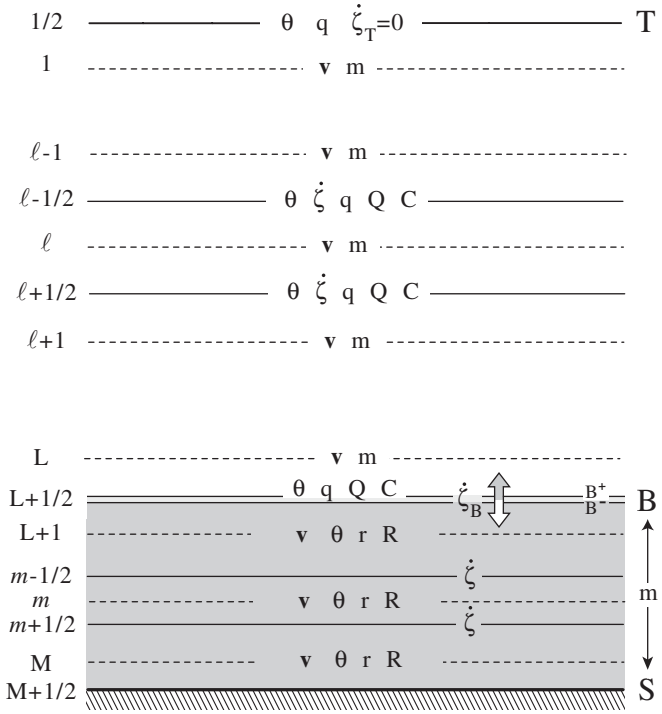

Fig. 3. Vertical grid used in the discretization.

Following Konor and Arakawa (2000), condensation rate C and condensation heating Q are calculated at the same level with θ and q. In the PBL, **v**, θ and total water mixing ratio r are predicted for the layers, as well as the rate of raindrop generation $\mathcal{R}$. The vertical mass flux at the top of the PBL, $\left(m\dot{\zeta}\right)_B$, is determined through the PBL parameterization.

5.b. Discrete equations for the free atmosphere

Mass continuity equation:

The vertically discrete version of the mass continuity equation (3.1) applied to the model layers within the free atmosphere is given by

$$\frac{\partial m_\ell}{\partial t} + \nabla\cdot\left(m\mathbf{v}\right)_\ell + \frac{1}{\left(\delta\zeta\right)_\ell}\left[\left(m\dot{\zeta}\right)_{\ell+1/2} - \left(m\dot{\zeta}\right)_{\ell-1/2}\right] = 0 \text{ for } \ell = 1,2,..,L\,, \qquad (5.1)$$

where

$$\left.\begin{aligned} m_\ell &= -(\delta p)_\ell/(\delta\zeta)_\ell \\ (\delta p)_\ell &= p_{\ell+1/2} - p_{\ell-1/2} \\ (\delta\zeta)_\ell &= \zeta_{\ell+1/2} - \zeta_{\ell-1/2} \end{aligned}\right\} \quad \text{for} \quad \ell = 1,2,...,L\,, \tag{5.2}$$

and $\left(m\dot{\zeta}\right)_{\ell+1/2}$ is the vertical mass flux carried at the interfaces of the model layers. Note that $(\delta\zeta)_\ell < 0$ in our indexing. We assume that, at the top of the atmosphere, $\left(m\dot{\zeta}\right)_{1/2} = 0$. The vertical mass flux at the PBL-top, $\left(m\dot{\zeta}\right)_{L+1/2}$, where $L+1/2$ and B are interchangeable, is determined by entrainment/detrainment parameterization. The vertically discrete pressure tendency equations can be obtained by vertically summing (5.1) with (5.2) as

$$\left.\begin{aligned} \frac{\partial p_{\ell+1/2}}{\partial t} &= \sum_{k=1}^{\ell} \nabla\cdot(m_k \mathbf{v}_k)(\delta\zeta)_k + \left(m\dot{\zeta}\right)_{\ell+1/2} \qquad \text{for} \quad \ell = 1,2,...,L \qquad (5.3a) \\ \frac{\partial p_B}{\partial t} &= \sum_{k=1}^{L} \nabla\cdot(m_k \mathbf{v}_k)(\delta\zeta)_k + \left(m\dot{\zeta}\right)_B, \qquad (5.3b) \end{aligned}\right\}$$

where we assumed that $\left(\partial p_T/\partial t\right) = 0$, where subscript $1/2$ and T are interchangeable.

Thermodynamic equation:

The vertically discrete version of the thermodynamic equation within the free atmosphere (3.4a) applied to the interfaces of the model layers are given by

$$\left.\begin{aligned} &\frac{\partial\theta_{1/2}}{\partial t} = 0 \qquad (5.4a) \\ &\frac{\partial\theta_{\ell+1/2}}{\partial t} + (\mathbf{v}\cdot\nabla\theta)_{\ell+1/2} + \left(\frac{\partial\theta}{\partial\zeta}\dot{\zeta}\right)_{\ell+1/2} = (Q/\Pi)_{\ell+1/2} \quad \text{for } \ell = 1,2,...,L-1 \qquad (5.4b) \\ &\frac{\partial\theta_{L+1/2}}{\partial t} + \mathbf{v}_L\cdot\nabla\theta_{L+1/2} + \left(\frac{\partial\theta}{\partial\zeta}\dot{\zeta}\right)_{L+1/2} = (Q/\Pi)_{L+1/2} \qquad (5.4c) \end{aligned}\right\}.$$

Equation (5.4a) is a result of choosing the upper boundary placed on an isentropic surface. In (5.4c), $\theta_{L+1/2}$ can be referred as to θ_{B^+}. In (5.4b) and (5.4c),

$$\left(\mathbf{v}\cdot\nabla\theta\right)_{\ell+1/2} \equiv \left[\frac{\Pi_{\ell+1}m_{\ell+1}\left(\delta\zeta\right)_{\ell+1}\mathbf{v}_{\ell+1}+\Pi_{\ell}m_{\ell}\left(\delta\zeta\right)_{\ell}\mathbf{v}_{\ell}}{\Pi_{\ell+1}m_{\ell+1}\left(\delta\zeta\right)_{\ell+1}+\Pi_{\ell}m_{\ell}\left(\delta\zeta\right)_{\ell}}\right]\cdot\nabla\theta_{\ell+1/2} \text{ for } \ell=1,2,...,L-1, \quad (5.4d)$$

$$\left(\frac{\partial\theta}{\partial\zeta}\dot{\zeta}\right)_{\ell+1/2} \equiv \frac{\Pi_{\ell+1/2}\left(\theta_{\ell+1}-\theta_{\ell}\right)}{\frac{1}{2}\left[\Pi_{\ell+1}m_{\ell+1}\left(\delta\zeta\right)_{\ell+1}+\Pi_{\ell}m_{\ell}\left(\delta\zeta\right)_{\ell}\right]}\left(m\dot{\zeta}\right)_{\ell+1/2} \quad \text{for} \quad \ell=1,2,...,L-1, \quad (5.4e)$$

where

$$\left.\begin{aligned}\Pi_{\ell} &\equiv \frac{\Pi_{\ell+1/2}p_{\ell+1/2}-\Pi_{\ell-1/2}p_{\ell-1/2}}{\left(\kappa+1\right)\left(p_{\ell+1/2}-p_{\ell-1/2}\right)}\\ \theta_{\ell} &\equiv \frac{1}{2}\left(\theta_{\ell+1/2}+\theta_{\ell-1/2}\right)\end{aligned}\right\} \quad \text{for} \quad \ell=1,2,...,L \quad (5.4f)$$

with $\Pi_{\ell+1/2}\equiv c_p\left(p_{\ell+1/2}/p_o\right)^{\kappa}$. In (5.4c), the vertical advection term is expressed by

$$\left(\frac{\partial\theta}{\partial\zeta}\dot{\zeta}\right)_{L+1/2} \equiv \frac{1}{m_{L+1/2}\left(\delta\zeta\right)_{L+1/2}}\left[\left(\hat{\theta}_{L+1/2}-\theta_{L+1/2}\right)\left(m\dot{\zeta}\right)_{L+1/2}+\left(\theta_{L+1/2}-\theta_{L}\right)\left(m\dot{\zeta}\right)_{L}\right], \quad (5.4g)$$

where $\hat{\theta}_{L+1/2}=\theta_{B^+}=\theta_{L+1/2}$ for $\left(m\dot{\zeta}\right)_{L+1/2}<0$ and $\hat{\theta}_{L+1/2}=\theta_{L+1}$ for $\left(m\dot{\zeta}\right)_{L+1/2}>0$. See Appendix A for the definition of $m_{L+1/2}$. Note that with (5.4g) we deviate from Konor and Arakawa (1997) by allowing vertical advection of the potential temperature at the lower boundary of the free atmosphere. When we consider only condensation process, heating Q can be written as

$$Q_{\ell+1/2}=LC_{\ell+1/2}. \quad (5.5)$$

Moisture equation:

From (3.6a) and (3.6b), the vertically discrete equations to predict the water vapor mixing ratio q within the free atmosphere are given by

$$\left.\begin{aligned}
&\frac{\partial(m q)_{1/2}}{\partial t} + \nabla\cdot(m q \mathbf{v})_{1/2} + \left[\frac{\partial}{\partial\zeta}\left(m q\dot{\zeta}\right)\right]_{1/2} = 0 && (5.6a)\\
&\frac{\partial(m q)_{\ell+1/2}}{\partial t} + \nabla\cdot(m q \mathbf{v})_{\ell+1/2} + \left[\frac{\partial}{\partial\zeta}\left(m q\dot{\zeta}\right)\right]_{\ell+1/2} = -(m C)_{\ell+1/2} \text{ for } \ell = 1,2,...,L && (5.6b)
\end{aligned}\right\}$$

The discrete moisture equations given by (5.6a) and (5.6b) are applied to the interfaces of the model layers following Konor and Arakawa (2000). With this choice, $C_{\ell+1/2}$ in (5.5) is identical to that in (5.6b) without any vertical averaging that decouples vertically smallest-scale condensation heating Q from condensation rate C. See Appendix A for the definition of $(m q \mathbf{v})_{\ell+1/2}$ in (5.6a) and (5.6b).

The divergence of vertical moisture fluxes in the moisture prediction equation given by (5.6a) and (5.6b) are defined by

$$\left.\begin{aligned}
&\left[\frac{\partial}{\partial\zeta}\left(m q\dot{\zeta}\right)\right]_{1/2} \equiv -\frac{1}{(\delta\zeta)_{1/2}} q_1 \left(m\dot{\zeta}\right)_{3/2} && (5.6c)\\
&\left[\frac{\partial}{\partial\zeta}\left(m q\dot{\zeta}\right)\right]_{\ell+1/2} \equiv \frac{1}{(\delta\zeta)_{\ell+1/2}}\left[q_{\ell+1}\left(m\dot{\zeta}\right)_{\ell+1} - q_\ell\left(m\dot{\zeta}\right)_{\ell}\right] \text{ for } \ell = 1,2,...,L-1 && (5.6d)\\
&\left[\frac{\partial}{\partial\zeta}\left(m q\dot{\zeta}\right)\right]_{L+1/2} \equiv \frac{1}{(\delta\zeta)_{L+1/2}}\left[\hat{q}_{L+1/2}\left(m\dot{\zeta}\right)_{L+1/2} - q_L\left(m\dot{\zeta}\right)_{L}\right] && (5.6e)
\end{aligned}\right\},$$

where $\hat{q}_{L+1/2} = q_{B^+} \equiv q_{L+1/2}$ for $\left(m\dot{\zeta}\right)_{L+1/2} < 0$ and $\hat{q}_{L+1/2} = q_{B^-} \equiv q_{L+1}$ for $\left(m\dot{\zeta}\right)_{L+1/2} > 0$. Note that q_{B^-} and q_{L+1} are within the PBL. In (5.6c) and (5.6d),

$$q_\ell \equiv \frac{q_{\ell+1/2} + q_{\ell-1/2}}{2} \text{ for } \ell = 1,2,...,L. \qquad (5.6d)$$

To avoid possible computational conditional instability, we will require that q_ℓ be bounded to satisfy $h_{\ell-1/2} \geq h_\ell \geq h_{\ell+1/2}$ or $h_{\ell-1/2} \leq h_\ell \leq h_{\ell+1/2}$, where the moist static energy is defined by $h \equiv \Pi\theta + \Phi + Lq$.

For a model with a low to moderate vertical resolution, the vertical discretization of the convergence of moisture fluxes given by (5.6c)-(5.6e) seems to be adequate. In a

model with high vertical resolution, however, this formulation may have computational problems such as overshooting and undershooting, especially near the PBL-top in simulating the processes during collapse of the PBL. We, therefore, use a different discretization in a high vertical resolution model, which produces better simulations of such processes. This formulation is discussed in detail in Appendix B.

Momentum equation:

The vertically discrete momentum equation applied to the model layers is given by

$$\frac{\partial \mathbf{v}_\ell}{\partial t} + \mathbf{v}_\ell \cdot \nabla \mathbf{v}_\ell + \left(\dot{\zeta}\frac{\partial \mathbf{v}}{\partial \zeta}\right)_\ell = -\left(\nabla_p \Phi\right)_\ell - f\,\mathbf{k}\times\mathbf{v}_\ell, \qquad (5.7a)$$

where **v** is the horizontal velocity, f is the Coriolis parameter; **k** is the unit vertical vector. The vertical advection of momentum is defined by

$$\left.\begin{aligned}
\left(\dot{\zeta}\frac{\partial \mathbf{v}}{\partial \zeta}\right)_1 &\equiv \frac{1}{2m_1(\delta\zeta)_1}(\mathbf{v}_2 - \mathbf{v}_1)\left(m\dot{\zeta}\right)_{3/2} && (5.7b)\\
\left(\dot{\zeta}\frac{\partial \mathbf{v}}{\partial \zeta}\right)_\ell &\equiv \frac{1}{2m_\ell(\delta\zeta)_\ell}\left[(\mathbf{v}_{\ell+1} - \mathbf{v}_\ell)\left(m\dot{\zeta}\right)_{\ell+1/2} + (\mathbf{v}_\ell - \mathbf{v}_{\ell-1})\left(m\dot{\zeta}\right)_{\ell-1/2}\right] && (5.7c)\\
& && \text{for } \ell = 2,3,\ldots,L-1 \quad (5.7d)\\
\left(\dot{\zeta}\frac{\partial \mathbf{v}}{\partial \zeta}\right)_L &\equiv \frac{1}{m_L(\delta\zeta)_L}\left[(\hat{\mathbf{v}}_{L+1/2} - \mathbf{v}_L)\left(m\dot{\zeta}\right)_B + \frac{1}{2}(\mathbf{v}_L - \mathbf{v}_{L-1})\left(m\dot{\zeta}\right)_{L-1/2}\right] && (5.7e)
\end{aligned}\right\},$$

where formally $\hat{\mathbf{v}}_{L+1/2} = \mathbf{v}_{B^+} \equiv f^+(\mathbf{v}_L, \mathbf{v}_{L-1})$ for $\left(m\dot{\zeta}\right)_B < 0$, which may be an extrapolation from above, and $\hat{\mathbf{v}}_{L+1/2} = \mathbf{v}_{B^-} \equiv f^-(\mathbf{v}_{L+2}, \mathbf{v}_{L+1})$ for $\left(m\dot{\zeta}\right)_B > 0$, which may be an extrapolation from PBL. Currently, we are using $\mathbf{v}_{B^+} \equiv \mathbf{v}_L$ and $\mathbf{v}_{B^-} \equiv \mathbf{v}_{L+1}$. The first term on the right hand side of (5.7a) is the pressure gradient force given by

$$-\left(\nabla_p \Phi\right)_\ell = -\nabla M_\ell + \Pi_\ell \nabla \theta_\ell, \qquad (5.8)$$

where $M_\ell \equiv \Pi_\ell \theta_\ell + \Phi_\ell$.

Hydrostatic equation:

The vertically discrete hydrostatic equation is given by

$$\Phi_\ell = \Phi_{\ell+1} + \left(\Pi_{\ell+1} - \Pi_{\ell+1/2}\right)\left(\theta_v\right)_{\ell+1} + \left(\Pi_{\ell+1/2} - \Pi_\ell\right)\left(\theta_v\right)_\ell \quad \text{for} \quad \ell = L, L-1, ..., 1\,, \quad (5.9)$$

where

$$\left(\theta_v\right)_\ell = \theta_\ell\left(1 + 0.608 q_\ell\right). \quad (5.10)$$

Vertical mass flux equation:

To derive the discrete vertical mass flux equation, we first vertically discetize the requirement (3.11) as

$$0 = \left(\frac{\partial}{\partial t}\right) F\left(\theta_{\ell+1/2}, \sigma_{\ell+1/2}\right) \quad \text{for} \quad \ell = 1, 2, .., L-1\,. \quad (5.11)$$

The right hand side of (5.11) may be written as

$$\left[\left(\frac{\partial F}{\partial \theta}\right)_\sigma \left(\frac{\partial \theta}{\partial t}\right)\right]_{\ell+1/2} +$$

$$\left[\left(\frac{\partial F}{\partial \sigma}\right)_\theta \left(\frac{\partial \sigma}{\partial p}\right)_{p_B}\right]_{\ell+1/2} \left(\frac{\partial p_B}{\partial t}\right) + \left[\left(\frac{\partial F}{\partial \sigma}\right)_\theta \left(\frac{\partial \sigma}{\partial p_B}\right)_p \left(\frac{\partial p}{\partial t}\right)\right]_{\ell+1/2} = 0 \quad \text{for} \quad \ell = 1, 2, ..L-1. \quad (5.12)$$

Using (5.3a), (5.3b) and (5.4b) with (5.4e) in (5.12), we obtain the generalized vertical mass flux equation as

$$\left(m\dot{\xi}\right)_{\ell+1/2} = \frac{\left(\frac{\partial}{\partial t}\right)_{\text{Horizontal}} F\left(\theta_{\ell+1/2}, \sigma_{\ell+1/2}\right)}{\left[\left(\frac{\partial F}{\partial \theta}\right)_\sigma \left(\frac{1}{m}\frac{\partial \theta}{\partial \xi}\right) - \left(\frac{\partial F}{\partial \sigma}\right)_\theta \left(\frac{\partial \sigma}{\partial p}\right)_{p_B}\right]_{\ell+1/2}} \quad \text{for} \quad \ell = 1, 2, ..., L-1 \quad (5.13a)$$

where

$$\left(\frac{\partial}{\partial t}\right)_{\text{Horizontal}} F\left(\theta_{\ell+1/2}, \sigma_{\ell+1/2}\right) \equiv \left[\left(\frac{\partial F}{\partial \theta}\right)_\sigma\right]_{\ell+1/2} \left[\left(Q/\Pi\right)_{\ell+1/2} - \left(\mathbf{v}\cdot\nabla\theta\right)_{\ell+1/2}\right]$$

$$+\left[\left(\frac{\partial F}{\partial \sigma}\right)_{\theta}\left(\frac{\partial \sigma}{\partial p}\right)_{p_B}\right]_{\ell+1/2}\sum_{k=1}^{\ell}\nabla\cdot(m_k\mathbf{v}_k)(\delta\zeta)_k$$

$$+\left[\left(\frac{\partial F}{\partial \sigma}\right)_{\theta}\left(\frac{\partial \sigma}{\partial p_B}\right)_{p}\right]_{\ell+1/2}\left(\sum_{k=1}^{L}\nabla\cdot(m_k\mathbf{v}_k)(\delta\zeta)_k+\left(m\dot{\zeta}\right)_B\right)\quad\text{for}\quad \ell=1,2,...,L-1. \qquad (5.13b)$$

In obtaining (5.13b), we used $\left(\partial p_T/\partial t\right)=0$. When $F\equiv\sigma_{\ell+1/2}$, $\left(m\dot{\zeta}\right)_B=0$ and $\dot{\zeta}_{\ell+1/2}=\dot{\sigma}_{\ell+1/2}$, (5.13.a) and (5.13b) yield

$$\left(m\dot{\sigma}\right)_{\ell+1/2}=-\nabla\cdot\sum_{k=1}^{\ell}(m\mathbf{v})_k(\delta\sigma)_k+\left(1-\sigma_{\ell+1/2}\right)\nabla\cdot\sum_{k=1}^{L}(m\mathbf{v})_k(\delta\sigma)_k, \qquad (5.14)$$

which is identical to the vertical mass flux for a σ coordinate. (Note that in our definitions of σ and $(\delta\sigma)_k$, $\dot{\sigma}>0$ when upward and $(\delta\sigma)_k<0$.) When $F\equiv\theta_{\ell+1/2}$ and $\dot{\zeta}_{\ell+1/2}=\dot{\theta}_{\ell+1/2}$, on the other hand, (5.13a) and (5.13b) yield

$$\dot{\theta}_{\ell+1/2}=\left(\frac{Q}{\Pi}\right)_{\ell+1/2}, \qquad (5.15)$$

which is the vertical mass flux equation for an isentropic coordinate. Time discretization of the vertical mass flux equation (5.13a) with (5.13b) will be discussed in subsection 10c.

5.c. Discrete equations for PBL

Mass continuity equation:

In a vertical coordinate based on the ζ coordinate for the PBL, the discrete version of the mass continuity equation (3.1) is

$$\frac{\partial m_{PBL}}{\partial t}+\frac{1}{(\delta\zeta)_{PBL}}\left[\sum_{m=L+1}^{M}\nabla\cdot(m\mathbf{v})_m(\delta\zeta)_m-\left(m\dot{\zeta}\right)_B\right]=0, \qquad (5.16)$$

where

$$\left.\begin{aligned} m_{PBL} &= -(\delta p)_{PBL}/(\delta\zeta)_{PBL} \\ (\delta p)_{PBL} &= p_{M+1/2} - p_{L+1/2} \\ (\delta\zeta)_{PBL} &= \zeta_{M+1/2} - \zeta_{L+1/2} \\ (\delta\zeta)_m &= \zeta_{m+1/2} - \zeta_{m-1/2} \quad \text{for} \quad m = L+1,...,M \end{aligned}\right\}. \tag{5.17}$$

The vertical mass flux at the PBL top, $(m\dot{\zeta})_{L+1/2}$, where $L+1/2$ and B are interchangeable, is determined by the bulk PBL parameterization. Note that $(\delta\zeta)_m < 0$ in our indexing. At the surface, $(m\dot{\zeta})_{M+1/2} = 0$, where $M+1/2$ and S are interchangeable. For convenience, we often omitted the subscript PBL in m_{PBL}. The vertically discrete pressure tendency equations can be obtained by vertically summing (5.16) with (5.17) within the free atmosphere as

$$\left.\begin{aligned} \frac{\partial p_{m+1/2}}{\partial t} &= \frac{\partial p_B}{\partial t} + \sum_{k=L+1}^{m} \nabla\cdot(m_k \mathbf{v}_k)(\delta\zeta)_k + (m\dot{\zeta})_{m+1/2} - (m\dot{\zeta})_B \text{ for } m = L+1,..,M-1 \quad (5.18a) \\ \frac{\partial p_S}{\partial t} &= \frac{\partial p_B}{\partial t} + \sum_{k=1}^{L} \nabla\cdot(m_k \mathbf{v}_k)(\delta\zeta)_k - (m\dot{\zeta})_B . \quad (5.18b) \end{aligned}\right\}$$

Thermodynamic equation:

The vertically discrete version of the thermodynamic equation (3.4b) applied to the individual layers is given by

$$\left.\begin{aligned} &\frac{\partial(m\theta)_{L+1}}{\partial t} + \nabla\cdot(m\mathbf{v}\theta)_{L+1} + \left[\frac{\partial(m\theta\dot{\zeta})}{\partial\zeta}\right]_{L+1} = \left(\frac{mQ}{\Pi}\right)_{L+1} - \frac{g}{(\delta\zeta)_{L+1}}(F_\theta)_{L+3/2} + (G_\theta)_{L+1} \quad (5.19a) \\ &\frac{\partial(m\theta)_m}{\partial t} + \nabla\cdot(m\mathbf{v}\theta)_m + \left[\frac{\partial(m\theta\dot{\zeta})}{\partial\zeta}\right]_m = \left(\frac{mQ}{\Pi}\right)_m - \frac{g}{(\delta\zeta)_m}\left[(F_\theta)_{m+1/2} - (F_\theta)_{m-1/2}\right] + (G_\theta)_m \\ &\qquad\qquad \text{for } m = L+2,...,M \quad (5.19b) \end{aligned}\right\}$$

where the subscript PBL is omitted in m_{PBL}. The convergence of vertical potential temperature fluxes is

$$\left.\begin{aligned}
\left[\frac{\partial}{\partial\zeta}\left(m\theta\dot{\zeta}\right)\right]_{L+1} &\equiv \frac{1}{\left(\delta\zeta\right)_{L+1}}\left[\theta_{L+3/2}\left(m\dot{\zeta}\right)_{L+3/2} - \hat{\theta}_{L+1/2}\left(m\dot{\zeta}\right)_{L+1/2}\right] && (5.19c)\\
\left[\frac{\partial}{\partial\zeta}\left(m\theta\dot{\zeta}\right)\right]_{m} &\equiv \frac{1}{\left(\delta\zeta\right)_{m}}\left[\theta_{m+1/2}\left(m\dot{\zeta}\right)_{m+1/2} - \theta_{m-1/2}\left(m\dot{\zeta}\right)_{m-1/2}\right] \\
& \qquad \text{for } m = L+2,\ldots,M-1 && (5.19d)\\
\left[\frac{\partial}{\partial\zeta}\left(m\theta\dot{\zeta}\right)\right]_{M} &\equiv -\frac{1}{\left(\delta\zeta\right)_{M}}\theta_{M-1/2}\left(m\dot{\zeta}\right)_{M-1/2} && (5.19e)
\end{aligned}\right\}$$

In (5.19c), we define $\hat{\theta}_{L+1/2} = \theta_{L+1/2} \equiv \theta_{B^+}$ for $\left(m\dot{\zeta}\right)_B < 0$ and $\hat{\theta}_{L+1/2} = \theta_{B^-} \equiv f^-\left(\theta_{L+2}, \theta_{L+1}\right)$ for $\left(m\dot{\zeta}\right)_B > 0$, which may be an extrapolation from PBL. Currently, we are using $\theta_{B^-} \equiv \theta_{L+1}$. In (5.19d) and (5.19e),

$$\theta_{m+1/2} \equiv \frac{\left(\Pi_{m+1} - \Pi_{m+1/2}\right)\theta_{m+1} + \left(\Pi_{m+1/2} - \Pi_m\right)\theta_m}{\left(\Pi_{m+1} - \Pi_m\right)} \text{ for } m = L+1,\ldots,M-1. \qquad (5.19f)$$

In (5.19a) and (5.19b), Q is diabatic heating rate per unit mass other than condensation and $\left(F_\theta\right)$ is the flux of θ due to convective eddies calculated from

$$\left.\begin{aligned}
\left(F_\theta\right)_{m+1/2} &= \frac{1}{\Pi_{m+1/2}}\left[\left(F_h\right)_{m+1/2} - L\left(F_r\right)_{m+1/2}\right] \quad \text{for an unsaturated level}\\
\left(F_\theta\right)_{m+1/2} &= \left(F_h\right)_{m+1/2} \Big/ \left[\Pi_{m+1/2}\left(1+\gamma_{m+1/2}\right)\right] \quad \text{for a saturated level}
\end{aligned}\right\}, \qquad (5.20a)$$

where $\gamma_{m+1/2} \equiv \frac{L}{c_p}\left[\left(\partial q^*/\partial T\right)_p\right]_{m+1/2}$, and F_h and F_r are convective eddy fluxes of moist static energy and total mixing ratio of water, respectively given by

$$\left.\begin{array}{l} \left.\begin{array}{l} h_{m+1/2} = \left(\Pi\theta + \Phi + Lq\right)_{m+1/2} \\ r_{m+1/2} \equiv q_{m+1/2} \end{array}\right\} \text{ for unsaturated air} \\ \left.\begin{array}{l} h_{m+1/2} = \left(\Pi\theta + \Phi + Lq^{*}\right)_{m+1/2} \\ r_{m+1/2} = q^{*}_{m+1/2} + \ell_{m+1/2} \end{array}\right\} \text{ for saturated air} \end{array}\right\}. \qquad (5.20b)$$

In (5.20.b), $\theta_{\ell+1/2}$ is defined by (5.19f), and the definitions of $\Phi_{\ell+1/2}$ and $r_{\ell+1/2}$ will be given later in this section. The expressions for $\left(F_h\right)_{m+1/2}$ and $\left(F_r\right)_{m+1/2}$ in (5.20a) are calculated from the bulk parameterization, which will be discussed later in this text. In (5.19a) and (5.19b), $\left(F_\theta\right)$ is formulated in the form of a difference of $\left(F_h\right)$ and $\left(F_r\right)$, which are the fluxes of two conserved quantities, h and r. This type of formulation is necessary because θ itself is not conserved during vertical mixing in a saturated atmosphere due to the release of condensation heating. In (5.19a) and (5.19b), $\left(G_\theta\right)$ represents the additional effects such as those due to the diffusive eddy fluxes and the roots of cumulus clouds. The formulation of $\left(G_\theta\right)$ will be discussed later in this text.

Moisture equation:

From the moisture continuity equation (3.6b), the vertically discrete equation to predict the water mixing ratio r is given by

$$\left.\begin{array}{l} \dfrac{\partial\left(mr\right)_{L+1}}{\partial t} + \nabla\cdot\left(mr\mathbf{v}\right)_{L+1} + \left[\dfrac{\partial}{\partial\zeta}\left(mr\dot{\zeta}\right)\right]_{L+1} = -m\mathcal{R}_{L+1} - \dfrac{g}{\left(\delta\zeta\right)_{L+1}}\left(F_r\right)_{L+3/2} + \left(G_r\right)_{L+1} \qquad (5.21a) \\ \dfrac{\partial\left(mr\right)_{m}}{\partial t} + \nabla\cdot\left(mr\mathbf{v}\right)_{m} + \left[\dfrac{\partial}{\partial\zeta}\left(mr\dot{\zeta}\right)\right]_{m} = -m\mathcal{R}_{m} - \dfrac{g}{\left(\delta\zeta\right)_{m}}\left[\left(F_r\right)_{m+1/2} - \left(F_r\right)_{m-1/2}\right] + \left(G_r\right)_{m} \\ \qquad\qquad m = L+1,\ldots,M \qquad (5.21b) \end{array}\right\}$$

where the subscript PBL is omitted in m_{PBL}. The convergence of vertical moisture fluxes is

$$\left.\begin{aligned}
\left[\frac{\partial}{\partial\zeta}\left(mr\dot{\zeta}\right)\right]_{L+1} &\equiv \frac{1}{(\delta\zeta)_{L+1}}\left[r_{L+3/2}\left(m\dot{\zeta}\right)_{L+3/2} - \hat{r}_{L+1/2}\left(m\dot{\zeta}\right)_{L+1/2}\right] && (5.21c)\\
\left[\frac{\partial}{\partial\zeta}\left(mr\dot{\zeta}\right)\right]_{m} &\equiv \frac{1}{(\delta\zeta)_{m}}\left[r_{m+1/2}\left(m\dot{\zeta}\right)_{m+1/2} - r_{m-1/2}\left(m\dot{\zeta}\right)_{m-1/2}\right] \text{ for } m = L+2,..,M-1 && (5.21d)\\
\left[\frac{\partial}{\partial\zeta}\left(mr\dot{\zeta}\right)\right]_{M} &\equiv -\frac{1}{(\delta\zeta)_{M}} r_{M-1/2}\left(m\dot{\zeta}\right)_{M-1/2} && (5.21e)
\end{aligned}\right\}$$

In (5.21c), we define $\hat{r}_{L+1/2} \equiv q_{L+1/2} = q_{B^+}$ for $\left(m\dot{\zeta}\right)_B < 0$ and $\hat{r}_{L+1/2} = r_{B^-} \equiv f^-\left(r_{L+2}, r_{L+1}\right)$ for $\left(m\dot{\zeta}\right)_B > 0$, which may be an extrapolation from PBL. Currently, we are using $r_{B^-} \equiv r_{L+1}$. In (5.21c) to (5.21e),

$$r_{m+1/2} \equiv \frac{r_{m+1} + r_m}{2} \text{ for } m = L+1,...,M-1. \qquad (5.21f)$$

To avoid possible computational conditional instability, we will require that $r_{m+1/2}$ be bounded to satisfy $h_m \geq h_{m+1/2} \geq h_{m+1}$ or $h_m \leq h_{m+1/2} \leq h_{m+1}$, where $h_{m+1/2}$ and $q_{m+1/2}$ are defined by (5.20b), $r_{m+1/2}$ is defined by (5.21f) and $\Phi_{m+1/2}$ will be defined later in this section. Note that the instability is unlikely to occur in the interior of the PBL since the layers are vertically mixed. On the other hand, it may occur at the top of the PBL and, therefore, r_{B^+}, which is formally $r_{B^+} \equiv q_{L+1/2}$, should be constrained.

In (5.21a) and (5.21b), $\left(F_r\right)$ and $\left(G_r\right)$ are analogous to the ones expressed for the potential temperature and $\mathcal{R}_m$ is the generation of raindrops. Note that, in the PBL, the total water-mixing ratio r is predicted instead of the water vapor mixing ratio q. The liquid water-mixing ratio ℓ is given by $r - q^*$, for $r > q^*$, and 0 for $r < q^*$. At present, the precipitation from the PBL is allowed only when the condensation level tends to be below the ground level. The total amount of precipitation is then determined to restore the condensation level to the ground level. The precipitation amount determined in this way is removed from each layer's r_m proportionally to their cloud mass $m\ell$. Turbulent flux of water-vapor mixing ratio $\left(F_q\right)_{m+1/2}$ is defined by

$$\left.\begin{aligned} \left(F_q\right)_{m+1/2} &= \left(F_r\right)_{m+1/2} && \text{for an unsaturated level} \\ \left(F_q\right)_{m+1/2} &= \gamma_{m+1/2}\left(F_h\right)_{m+1/2}\Big/\left[L\left(1+\gamma_{m+1/2}\right)\right] && \text{for a saturated level} \end{aligned}\right\}. \qquad (5.21g)$$

Momentum equation:

From (3.7b), the vertically discrete momentum equation applied to the individual layers identified by m is given by

$$\left.\begin{aligned} &\frac{\partial \mathbf{v}_{L+1}}{\partial t} + \mathbf{v}_{L+1}\cdot\nabla\mathbf{v}_{L+1} + \left\{\dot{\zeta}\frac{\partial \mathbf{v}}{\partial \zeta}\right\}_{L+1} = \\ &\qquad -\left(\nabla_p\Phi\right)_{L+1} - f\,\mathbf{k}\times\mathbf{v}_{L+1} - \frac{g}{m_{PBL}\left(\delta\zeta\right)_{L+1}}\left(\mathbf{F}_v\right)_{L+3/2} + \frac{\left(\mathbf{G}_v\right)_{L+1}}{m_{PBL}} \qquad (5.22a) \\ &\frac{\partial \mathbf{v}_m}{\partial t} + \mathbf{v}_m\cdot\nabla\mathbf{v}_m + \left\{\dot{\zeta}\frac{\partial \mathbf{v}}{\partial \zeta}\right\}_m = \\ &\qquad -\left(\nabla_p\Phi\right)_m - + f\,\mathbf{k}\times\mathbf{v}_m - \frac{g}{m_{PBL}\left(\delta\zeta\right)_m}\left\{\left(\mathbf{F}_v\right)_{m+1/2} - \left(\mathbf{F}_v\right)_{m-1/2}\right\} + \frac{\left(\mathbf{G}_v\right)_m}{m_{PBL}} \\ &\qquad\qquad m = L+2,\ldots,M \qquad (5.22b) \end{aligned}\right\},$$

where the vertical momentum advection is

$$\left.\begin{aligned} \left\{\dot{\zeta}\frac{\partial \mathbf{v}}{\partial \zeta}\right\}_{L+1} &\equiv \frac{1}{m\left(\delta\zeta\right)_{L+1}}\left[\frac{1}{2}\left(\mathbf{v}_{L+2}-\mathbf{v}_{L+1}\right)\left(m\dot{\zeta}\right)_{L+3/2} + \left(\mathbf{v}_{L+1}-\hat{\mathbf{v}}_{L+1/2}\right)\left(m\dot{\zeta}\right)_B\right] \qquad (5.22c) \\ \left\{\dot{\zeta}\frac{\partial \mathbf{v}}{\partial \zeta}\right\}_m &\equiv \frac{1}{2m\left(\delta\zeta\right)_m}\left[\left(\mathbf{v}_{m+1}-\mathbf{v}_m\right)\left(m\dot{\zeta}\right)_{m+1/2} + \left(\mathbf{v}_m-\mathbf{v}_{m-1}\right)\left(m\dot{\zeta}\right)_{m-1/2}\right] \\ &\qquad\qquad \text{for } m = L+1,..,M-1 \qquad (5.22d) \\ \left\{\dot{\zeta}\frac{\partial \mathbf{v}}{\partial \zeta}\right\}_M &\equiv \frac{1}{2m\left(\delta\zeta\right)_M}\left(\mathbf{v}_M-\mathbf{v}_{M-1}\right)\left(m\dot{\zeta}\right)_{M-1/2} \qquad (5.22e) \end{aligned}\right\},$$

where the subscript PBL is omitted in m_{PBL}. In (5.22c), we formally define $\hat{\mathbf{v}}_{L+1/2} = \mathbf{v}_{B^+} \equiv f^+\left(\mathbf{v}_L, \mathbf{v}_{L-1}\right)$ for $\left(m\dot{\zeta}\right)_B < 0$, which may be an extrapolation from above,

and $\hat{\mathbf{v}}_{L+1/2} = \mathbf{v}_{B^-} \equiv f^-\left(\mathbf{v}_{L+2}, \mathbf{v}_{L+1}\right)$ for $\left(\dot{m\xi}\right)_B > 0$, which may be an extrapolation from PBL. Currently, we are using $\mathbf{v}_{B^+} \equiv \mathbf{v}_L$ and $\mathbf{v}_{B^-} \equiv \mathbf{v}_{L+1}$. On the right hand side (5.22a) and (5.22b), $-\left(\nabla\Phi\right)_{L+1}$ and $-\left(\nabla\Phi\right)_m$ are the vertically discrete version of the pressure gradient force (3.8), and $\left(\mathbf{F}_\mathbf{v}\right)_{L+3/2}$ and $\left(\mathbf{F}_\mathbf{v}\right)_{m+1/2}$ are the convergence of the convective eddy fluxes of momentum. In (5.22a) and (5.22b), $\left(\mathbf{G}_\mathbf{v}\right)_{L+3/2}$ and $\left(\mathbf{G}_\mathbf{v}\right)_{m+1/2}$ represent the additional effects such as those due to diffusive eddy fluxes and roots of cumulus clouds. Formulations of these terms will be discussed later in this text. The vertically discrete pressure gradient force is

$$-\left(\nabla_p\Phi\right)_m = -\nabla M_m + \Pi_m \nabla\theta_m , \tag{5.23}$$

where $M_m \equiv \Pi_m\theta_m + \Phi_m$. An alternative discrete form for (5.23) is given in Appendix C.

Hydrostatic equation:

The vertically discrete version of the hydrostatic equation (3.9), which is used to determine the geopotential Φ_m within the PBL, is

$$\left.\begin{aligned} \Phi_m &= \Phi_{m+1} + \left(\Pi_{m+1} - \Pi_{m+1/2}\right)\left(\theta_v\right)_{m+1} + \left(\Pi_{m+1/2} - \Pi_m\right)\left(\theta_v\right)_m \text{ for } m = M-1,..L+1 && (5.24a)\\ \Phi_M &= \Phi_S + \left(\Pi_S - \Pi_M\right)\left(\theta_v\right)_M && (5.24b)\end{aligned}\right\}$$

where

$$\left.\begin{aligned} \Pi_{m+1/2} &\equiv c_p\left(\frac{p_{m+1/2}}{p_o}\right)^{R/c_p} && (5.24c)\\ \Pi_m &\equiv c_p\left(\frac{p_m}{p_o}\right)^{R/c_p} && (5.24d)\\ \Pi_m &\equiv \frac{p_{m+1/2}\Pi_{m+1/2} - p_{m-1/2}\Pi_{m-1/2}}{\left(R/c_p + 1\right)\left(p_{m+1/2} - p_{m-1/2}\right)} && (5.24e)\\ \left(\theta_v\right)_m &\equiv \theta_m\left(1 + 0.608q_m\right) && (5.24f)\end{aligned}\right\}.$$

Vertical mass flux equation:

As we stated earlier, we use a sigma-type coordinate for the PBL defined by $\zeta \equiv F^*(\sigma^*) = \zeta_B + (\zeta_S - \zeta_B)(\sigma^* - \sigma_B^*)(\sigma_S^* - \sigma_B^*)^{-1}$, where $\sigma^* \equiv (p_S - p)(p_S - p_B)^{-1}$, ζ_B is determined from the lowest value of ζ for the free atmosphere, and $\zeta_S = \gamma \zeta_B$, where γ is an arbitrarily prescribed constant less than 1. Then, from (3.18), we can obtain the discrete vertical mass flux equation within the PBL as

$$\left(m\dot{\zeta}\right)_{m+1/2} = \frac{\left(\zeta_S - \zeta_{m+1/2}\right)}{\left(\zeta_S - \zeta_B\right)}\left(m\dot{\zeta}\right)_B - \sum_{k=L+1}^{m} \nabla\cdot(m\mathbf{v})_k (\delta\zeta)_k + \frac{\left(\zeta_{m+1/2} - \zeta_B\right)}{\left(\zeta_S - \zeta_B\right)} \sum_{m=L+1}^{M} \nabla\cdot(m\mathbf{v})_k (\delta\zeta)_k$$

for $m = L+1,\ldots,M-1$. (5.25)

The PBL-top vertical mass flux is calculated by

$$\left(m\dot{\zeta}\right)_B = -g\left(E - D - M_B\right), \tag{5.26}$$

where $E > 0$ (and $D = 0$) represents entrainment, $D > 0$ (and $E = 0$) represents detrainment, and $M_B > 0$ is the total upward flux across the PBL due to cumulus convection. E and D are determined by the bulk parameterization discussed later in this text.

6-Discretization of PBL processes

Turbulence fluxes due to large convective eddies:

It is assumed that the turbulence fluxes of $\mathbf{v}$, h and r due to large convective eddies change linearly in the vertical within PBL. If ψ represents $\mathbf{v}$, h or r, the flux at a certain level within the PBL can be written as

$$\left(F_\psi\right)_{m+1/2} = \frac{\zeta_B - \zeta_{m+1/2}}{\zeta_B - \zeta_S}\left(F_\psi\right)_S + \frac{\zeta_{m+1/2} - \zeta_S}{\zeta_B - \zeta_S}\left(F_\psi\right)_{B^-} \quad \text{for } m = L+1, \cdots, M-1, \quad (6.1)$$

where $\left(F_\psi\right)_S$ and $\left(F_\psi\right)_{B^-}$ are the surface and PBL-top fluxes at level B^- of ψ determined by the bulk parameterization discussed later in this text. Note that B^- denotes the lower boundary of an infinitesimally thin fictitious transition layer identified by B. A detailed discussion on the budget of ψ near the PBL-top is presented later in this section and in Appendix D.

Turbulence fluxes due to small diffusive eddies:

In the PBL parameterization described here, we include the effects of internal diffusion due to small eddies. We can write those fluxes as

$$\left.\begin{aligned} &\left(\tilde{F}_\psi\right)_{L+1/2} \equiv 0 \\ &\left(\tilde{F}_\psi\right)_{m+1/2} \equiv \frac{\rho_{m+1/2} K_{m+1/2}}{\left(\delta z\right)_{m+1/2}}\left(\psi_{m+1} - \psi_m\right) \text{ for } m = L+1, \cdots, M-1 \\ &\left(\tilde{F}_\psi\right)_{M+1/2} \equiv 0 \end{aligned}\right\}, \quad (6.2)$$

where ψ represents $\mathbf{V}$, h or r. In (6.2), $\rho_{m+1/2}$ is the density, $K_{m+1/2}$ is the diffusion coefficient and $\left(\delta z\right)_{m+1/2} \equiv z_m - z_{m+1}$. The diffusive fluxes of the potential temperature can be written as

$$\left.\begin{aligned} \left(\tilde{F}_\theta\right)_{m+1/2} &= \frac{1}{\Pi_{m+1/2}}\left[\left(\tilde{F}_h\right)_{m+1/2} - L\left(\tilde{F}_q\right)_{m+1/2}\right] \quad \text{for an unsaturated level} \\ \left(\tilde{F}_\theta\right)_{m+1/2} &= \left(\tilde{F}_h\right)_{m+1/2} \Big/ \left[\Pi_{m+1/2}\left(1 + \gamma_{m+1/2}\right)\right] \quad \text{for a saturated level} \end{aligned}\right\}. \quad (6.3)$$

Note that, for an unsaturated level, $\left(\tilde{F}_q\right)_{m+1/2} = \left(\tilde{F}_r\right)_{m+1/2}$.

Fluxes due to cumulus convection and radiation:

The budget of an arbitrary quantity ψ is also modified by the cumulus mass flux and, when relevant, radiation flux of ψ in or out of the PBL. They primarily affect the budgets in the top layer of the PBL through

$$\left(\frac{\partial}{\partial t}\right)_{\text{partial}} (m\psi)_{L+1} = -\frac{g}{(\delta\zeta)_{L+1}}\left[\left(\psi_{B^+} - \psi_{B^-}\right)M_B - \left(R_\psi\right)_{B^+}\right], \qquad (6.4)$$

where $\psi_{B^-} \equiv f^-\left(\psi_{L+1}, \psi_{L+2}\right)$, and $\psi_{B^+} \equiv \psi_{L+1/2}$ for $\psi \equiv \theta$ and $\psi \equiv r$, and $\psi_{B^+} \equiv f^+\left(\psi_{L-1}, \psi_L\right)$ for $\psi \equiv \mathbf{v}$. In (6.4), $\left(R_\psi\right)_{B^+}$ is the upward radiation flux of ψ at B^+ with $\left(R_{\mathbf{v}}\right)_{B^+} = \left(R_r\right)_{B^+} = 0$. A detailed derivation of (6.4) is given in Appendix D.

The effect of cumulus roots can be incorporated into this formulation by redistributing $\left(\psi_{B^+} - \psi_{B^-}\right)M_B$ in (6.4), into the all PBL layers including a fraction of the flux $\lambda_m^{(c)}\left(\psi_{B^+} - \psi_{B^-}\right)M_B$ to the budget equations, where $\lambda_m^{(c)}$ is the fractional contribution to the cumulus flux from layer m satisfying $\sum_{m=L+1}^{M} \lambda_m^{(c)} = 1$.

We sum the effects discussed in this section in one term as

$$\left.\begin{aligned}
\left(G_\psi\right)_m &\equiv \frac{-g}{(\delta\zeta)_m}\left[\left(\tilde{F}_\psi\right)_{m+1/2} - \left(\tilde{F}_\psi\right)_{m-1/2} + \lambda_m^{(c)}\left(\psi_{B^+} - \psi_{B^-}\right)M_B\right] \quad \text{for } m = L+2, \cdots, M \\
\left(G_\psi\right)_{L+1} &\equiv \frac{-g}{(\delta\zeta)_{L+1}}\left[\left(\tilde{F}_\psi\right)_{L+3/2} + \lambda_{L+1}^{(c)}\left(\psi_{B^+} - \psi_{B^-}\right)M_B - \left(R_\psi\right)_{B^+}\right]
\end{aligned}\right\} . \qquad (6.5)$$

7. Bulk PBL parameterization

Here we describe a recently introduced bulk parameterization of the PBL by Randall, Branson, Zhang, Moeng and Krasner (unpublished manuscript), which is essentially an extension of the approach followed by Suarez et al. (1983). In this parameterization, i) the bulk turbulence kinetic energy (TKE) for the PBL is predicted, ii) the square-root of the predicted TKE is used for the bulk velocity in determining the surface fluxes, and iii) an explicit formulation based on the predicted TKE is used to determine the PBL-top entrainment rate. Additionally, this parameterization has a simplified PBL-top entrainment instability formulation, which is incorporated into the expression that determines the entrainment rate.

As in Suarez et al. (1983), we consider three regimes for the PBL as schematically shown in Fig. 4. The first regime is the clear deepening PBL such as clear daytime PBL over land. In this regime, the TKE increases typically due to the buoyancy generated by the warming of Earth's surface due to solar heating, and consequently the PBL tends to deepen by entraining air from the free atmosphere. The second regime is the night-time situation over land. After sunset, due to the sudden loss of the buoyancy generation, the TKE decreases and then the PBL collapses, leaving a large part of PBL air to the free atmosphere. Unlike the deepening PBL case, there is no well-defined PBL top during this

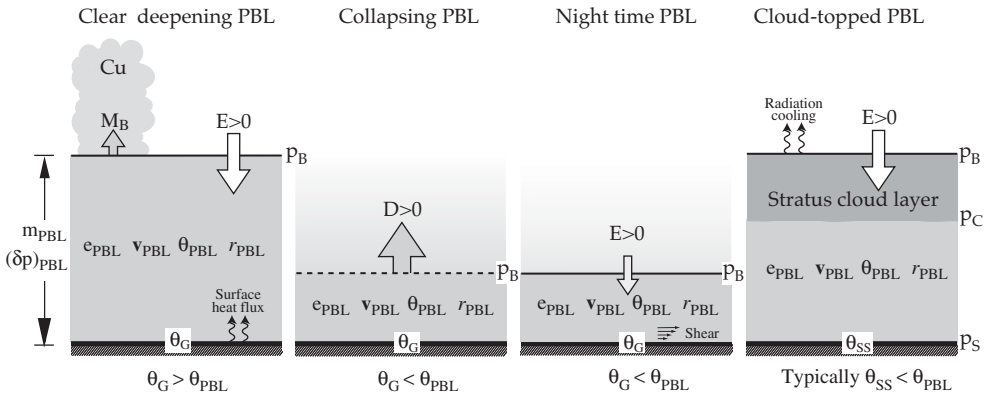

Fig. 4. Schematic representation of the different PBL regimes considered in the PBL parameterization. The subscripts G and SS denote ground and sea surface, respectively, and they can be used interchangeably.

transition, which is this difficult to simulate in a discrete model. Yet, this process is an essential part of the PBL-free atmosphere interaction. For that reason, we pay a special care on realistically simulating this process in our model. The technique we used will be discussed later in this text. After this transition, the PBL typically starts deepening again with a relatively slow rate due to the shear contribution to the TKE generation during the night time. In the parameterization we also consider the cloud-topped PBL regime, which is often observed over the colder oceans of the cost of California and Peru and over the high-latitude snow-covered land. In this regime, the TKE is maintained by the buoyancy generated by radiative cooling near the top of the cloud layer.

Determination of bulk quantities for multi layer PBL

Suarez et al. (1983) predicts the PBL velocity, the potential temperature and the total water mixing ratio for the *sub-cloud layer* of the PBL. Unlike their parameterization, here we predict the velocity $\mathbf{V}_m$, potential temperature θ_m, total water mixing ratio r_m for each of the multiple layers within the PBL identified by $m = L+1,...,M$. Therefore, we must define the bulk properties to be used in the bulk parameterization in terms of these predicted quantities. We define a bulk value of ψ denoted by ψ_{PBL} as

$$\psi_{PBL} \equiv \frac{1}{\int_{p_B}^{p_S} \eta dp} \int_{p_B}^{p_S} \eta\psi(p)dp, \tag{7.1}$$

where

$$\eta = \begin{cases} 1 & \text{for} \quad r < q^*(T,p) \\ 0 & \text{for} \quad r \geq q^*(T,p) \end{cases}. \tag{7.2}$$

If the entire PBL is saturated, we define $\psi_{PBL} = \psi(p_S)$. In the discrete system, we use (7.1) and (7.2) applied to vertically interpolated (linearly in Π) ψ, θ and r from the layers identified by $m = L+1,...,M$.

Turbulence kinetic energy equation

The bulk turbulence kinetic energy (TKE) for the mixed-layer e_{PBL} is predicted by

$$\frac{\partial e_{PBL}}{\partial t} = -\frac{e_{PBL}}{(\delta p)_{PBL}} gE + \frac{g}{(\delta p)_{PBL}}(\mathcal{B} + S - \mathcal{D}) + \frac{e_{PBL}}{m}\nabla\cdot(m\mathbf{v}), \tag{7.3}$$

where $(\delta p)_{PBL} = p_S - p_B$, E is the entrainment rate satisfying $gE = -\left(m\dot{\zeta}\right)_B$ for $M_B = 0$, $\mathcal{B}$ is the buoyancy generation, S is the shear generation, $\mathcal{D}$ is the dissipation of TKE and m is the mass of the PBL defined by $m \equiv (\delta p)_{PBL} / (\zeta_{L+1/2} - \zeta_{M+1/2})$. The derivation of (7.3) is discussed in Appendix E. The buoyancy generation is given by

$$\mathcal{B} \equiv \int_{p_B}^{p_S} \frac{\kappa F_{sv}}{p} dp, \tag{7.4}$$

where $\kappa \equiv R/c_p$. In (7.4), F_{sv} is the turbulent flux of virtual dry static energy $s_v = \Pi\theta_v + \Phi$, where θ_v is the virtual potential temperature, which is defined by $\theta_v \equiv T_v(p/p_o)^\kappa$. T_v is the virtual temperature is given by $T_v \equiv T(1 + 0.608\,q - \ell)$, where q and ℓ are the mixing ratios of water vapor and liquid water, respectively. The shear generation is formally given by

$$S \equiv \int_{z_S}^{z_B} \mathbf{F_v} \cdot \frac{\partial \mathbf{v}}{\partial z} dz, \tag{7.5}$$

where $\mathbf{F_v}$ is the turbulent momentum flux. In our model, however, we only consider low-level shear to calculate S, which will be discussed later in this text. The dissipation of TKE in (7.3) is expressed by

$$\mathcal{D} \equiv C\rho_{PBL}\left(e_{PBL}\right)^{3/2}, \tag{7.6}$$

In (7.6), C is a constant, which remains to be determined and ρ_{PBL} is the averaged density in the PBL given by $\rho_{PBL} \equiv \left(\delta p\right)_{PBL} / g\left(z_B - z_S\right)$.

Equation (7.3) is valid only for the "turbulent (deepening) state", for which formally $e_{PBL} > 0$ (in our model, $e_{PBL} > e_{min}$). If there is a tendency toward $e_{PBL} < e_{min}$, it is assumed that the mixed-layer is in "collapsing state", for which we let $e_{PBL} = e_{min}$ and $\left(\delta p\right)_{PBL} = \left(\delta p\right)_{min}$, where e_{min} and $\left(\delta p\right)_{min}$ are properly chosen lower limits of e_{PBL} and $\left(\delta p\right)_{PBL}$, respectively. The PBL maintains the "collapsed state" until $e_{PBL} > e_{min}$ again.

Surface fluxes:

Surface fluxes are given by

$$\left.\begin{aligned}
\left(\mathbf{F_v}\right)_S &\equiv -\rho_S C_M \, F\left(\sqrt{e_{PBL}}, \left|\tilde{\mathbf{v}}_{PBL}\right|\right) \tilde{\mathbf{v}}_{PBL} \\
\left(F_\theta\right)_S &\equiv \rho_S C_T \, F\left(\sqrt{e_{PBL}}, \left|\tilde{\mathbf{v}}_{PBL}\right|\right) \left(\theta_S - \theta_{PBL}\right) \\
\left(F_r\right)_S &\equiv \rho_S C_r \beta_W\left(W'\right) F\left(\sqrt{e_{PBL}}, \left|\tilde{\mathbf{v}}_{PBL}\right|\right) \left(q^*\left(T_S, p_S\right) - q_{PBL}\right)
\end{aligned}\right\}, \tag{7.7}$$

We are inspired by the work by Stull (1988), Zhang et al. (1996) and Deardorff (1972) for selecting these forms. In (7.7), C_M, C_T and C_r are the surface transfer coefficients for their respected fields. In the calculation of $\left(\mathbf{F_v}\right)_S$, we use the lowest PBL layer velocity, $\hat{\mathbf{v}}_{PBL} \equiv \mathbf{v}_M$. $\beta_W\left(W'\right)$ is the availability of water for evaporation from the surface and W' is a measure of wetness (see Suarez et al.,1983). In the original formulation suggested by RBZMK, the heat transfer coefficient C_T is determined as a function of $\left(\mathcal{V}_\theta\right)_{PBL} / \left(\theta_S - \theta_{PBL}\right)^2$, where the bulk turbulence variance of the potential temperature $\left(\mathcal{V}_\theta\right)_{PBL}$ is predicted through an equation analogous to (7.3). The momentum transfer

coefficient C_M is determined as a function of $e_{PBL}/|\mathbf{v}_{PBL}|^2$ and a bulk Richardson number in such a way that C_M reduces to a function of $e_{PBL}/|\mathbf{v}_{PBL}|^2$ for a neutral PBL. Then RBZMK suggests incorporation of surface roughness formulation into C_M. In our very early applications, we followed the procedure suggested by RBZMK in which the bulk variances are predicted and then the transfer coefficients are calculated. Our tests showed, however, too large variability in the calculated transfer coefficients. When we applied upper and lower bounds, the values for the transfer coefficients flip-flopped between two bounds every other time step. Therefore, we postponed the implementation of this procedure using constant values in the order of 10^{-3} for the transfer coefficients. (In the GCM applications, Deardorff's (1972) formulations must be used instead of the constant transfer coefficients.)

In (7.7), we define the velocity scale as a function of the square-root of bulk TKE and grid-scale surface wind through the use of $F\left(\sqrt{e_{PBL}},|\mathbf{v}_M|\right)$, where $\mathbf{v}_M$ is the grid-scale wind at the lowest layer of the PBL. Inclusion of $\mathbf{v}_M$ is needed to obtain realistic surface fluxes in the middle latitudes where surface wind is generally strong. In the formulation used for the simulations presented in this paper, we selected $F\left(\sqrt{e_{PBL}},|\mathbf{v}_M|\right) \equiv \sqrt{e_{PBL}} + 0.25|\mathbf{v}_M|$. (In the GCM application of this parameterization, however, $F\left(\sqrt{e_{PBL}},|\mathbf{v}_M|\right) \equiv \text{Max}\left\{\sqrt{e_{PBL}},|\mathbf{v}_M|\right\}$ is used.)

Determination of the bulk turbulence fluxes, buoyancy generation and PBL top entrainment rate:

a) Clear deepening PBL (typically $\theta_G > \theta_{PBL}$):

Typical vertical profiles of r, q, θ, s, h and h* are shown in Fig. 5 for clear deepening PBL. Here r = q and the dry static energy is defined by $s \equiv \Pi\theta + \Phi$.

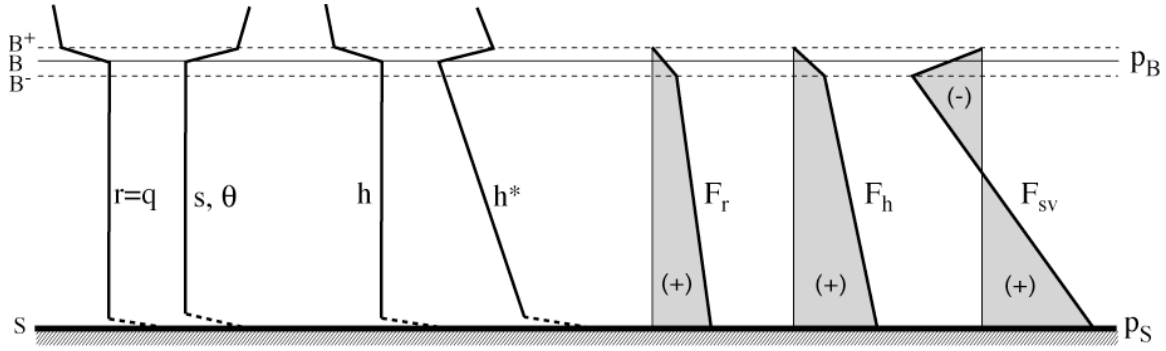

Fig. 5. Typical vertical profiles of r, q, θ, s, h, h*, F_r, F_h and F_{sv} for clear deepening PBL.

Within the PBL, the conserved quantities, namely r, θ, s and h, are vertically well mixed while h* decreases nearly linearly with height. The turbulence fluxes of the total water F_r and moist static energy F_h given by $\Pi F_\theta + LF_r$, where $\Pi F_\theta = F_s$, are positive and linearly decreases with height from their surface values, $\left(F_r\right)_S$ and $\left(F_h\right)_S = \Pi_S\left(F_\theta\right)_S + L\left(F_r\right)_S$, respectively. The surface fluxes $\left(F_\theta\right)_S$ and $\left(F_r\right)_S$ are given by (7.7) and the PBL-top fluxes are given by

$$\left.\begin{aligned}\left(F_r\right)_{B^-} &= -E\left(\Delta r\right)_B \\ \left(F_h\right)_{B^-} &= -E\left(\Delta h\right)_B\end{aligned}\right\}, \tag{7.8}$$

where $\left(\Delta\ \right)_B \equiv \left(\ \ \right)_{B^+} - \left(\ \ \right)_{B^-}$. In (7.8), the PBL-top fluxes, $\left(F_r\right)_{B^-}$ and $\left(F_h\right)_{B^-}$ are found from (D.4) of Appendix D by requiring $\left(\Delta R_r\right)_B = \left(\Delta R_h\right)_B = 0$ for clear PBL case and neglecting M_B. The turbulence flux of the virtual dry static energy F_{sv}, which is given by $F_h + \left(0.608\Pi\theta_{PBL} - L\right)F_r$ or $\Pi F_\theta + 0.608\Pi\theta_{PBL}F_r$, linearly decreases with height from a positive value at the surface, $\left(F_{sv}\right)_S > 0$, to a negative value at the PBL-top, $\left(F_{sv}\right)_{B^-} < 0$. There is a well-established empirical relationship between $\left(F_{sv}\right)_S$ and $\left(F_{sv}\right)_{B^-}$ given by

$$\left(F_{sv}\right)_{B^-} = -k\left(F_{sv}\right)_S, \tag{7.9}$$

where $k \approx 0.2$. The buoyancy generation (7.4) for this case can be written as

$$\mathcal{B} \approx \kappa\left[\left(F_{sv}\right)_S + \left(F_{sv}\right)_{B^-}\right]\left(p_S - p_B\right)/\left(p_S + p_B\right), \tag{7.10}$$

where $\kappa \equiv R/c_p$ and

$$\left.\begin{aligned}\left(F_{sv}\right)_{B^-} &= \left(F_h\right)_{B^-} + \left(0.608\Pi_B\theta_{PBL} - L\right)\left(F_r\right)_{B^-} = \Pi_B\left(F_\theta\right)_{B^-} + 0.608\Pi_B\theta_{PBL}\left(F_r\right)_{B^-} \\ \left(F_{sv}\right)_S &= \left(F_h\right)_S + \left(0.608\Pi_S\theta_{PBL} - L\right)\left(F_r\right)_S = \Pi_S\left(F_\theta\right)_S + 0.608\Pi_S\theta_{PBL}\left(F_r\right)_S\end{aligned}\right\}, \quad (7.11)$$

where we used $\Pi_B\left(F_\theta\right)_{B^-} = \left(F_\theta\right)_{B^-} - L\left(F_r\right)_{B^-}$ and $r \equiv q$. Following Randall, Branson, Zhang, Moeng and Krasner (unpublished manuscript), the PBL-top entrainment is determined from

$$E \approx \left(\frac{2kC}{1-k}\right)\frac{\rho_{PBL}\sqrt{\tilde{e}_{PBL}}}{\dfrac{g\left(\Delta s_v\right)_B\left(\delta z\right)_{PBL}}{e_{PBL}\Pi_B\theta_{PBL}}}, \quad (7.12)$$

where $\tilde{e}_{PBL} \equiv e_{PBL} - e_{min}$. We assume that $\left(\Delta s_v\right)_B = \Pi_B\left(\Delta\theta\right)_B + 0.608\left(\Delta r\right)_B$ is positive and use the typical value of $C \approx 1$ (see Moeng and Sullivan, 1994).

b) Collapsing PBL (typically $\theta_G < \theta_{PBL}$):

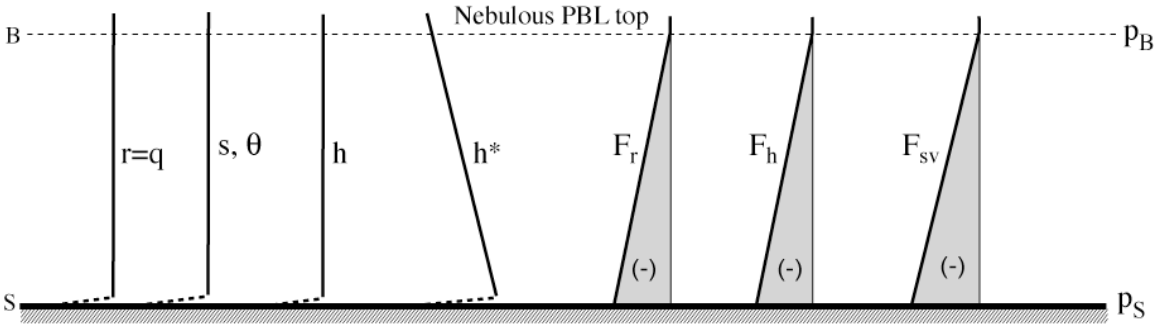

Fig. 6. Typical vertical profiles of r, q, θ, s, h , h*, F_r, F_h and F_{sv} for collapsing PBL.

For the collapsing case, the TKE is nearly zero and, therefore, the PBL is not well defined so that we choose $\left(\Delta h\right)_B = \left(\Delta r\right)_B = 0$. The turbulence fluxes are typically negative (see Fig. 6). In our model, we assume that the PBL air detrains through its prognostically determined top with a finite rate while the TKE is set to its minimum value, $e_{PBL} = e_{min}$. The detrainment rate D is calculated from an arbitrary relationship given by

$$D \equiv \frac{\left(\delta p\right)_{max}}{g\tau_{collapse}}, \quad (7.13)$$

Where we use values for $(\delta p)_{max}$ and $\tau_{collapse}$ given by 250 mb and 3 hours, respectively.

c) $\theta_G < \theta_{PBL}$ (Nighttime PBL):

After the collapse of the PBL, the TKE starts increasing again due to the shear contribution. We treat this regime similar to the clear deepening PBL except the TKE here is generated by the shear rather than the buoyancy.

d) Cloud-topped PBL (typically $\theta_{SS} < \theta_{PBL}$):

A cloud layer forms in the upper PBL if the condensation level denoted by C is lower than the PBL-top. The height of the condensation level can be determined by

$$p_C \equiv p_B + (p_S - p_B)\frac{r_{PBL} - q^*_{B0}}{q^*_S - q^*_{B0}}, \qquad (7.14)$$

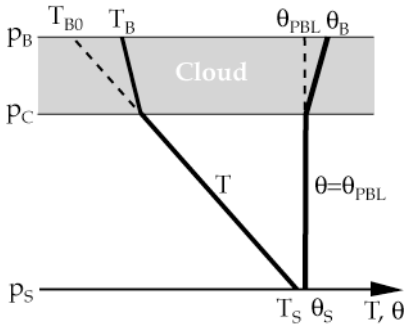

Fig. 7. Typical vertical profiles of the temperature T and the potential temperature θ in a cloud-topped PBL.

where $q^*_S = q^*(T_S, p_S)$, $q^*_{B0} = q^*(T_{B0}, p_B)$, $T_S \equiv \Pi_S \theta_{PBL}/c_p$ and $T_{B0} \equiv \Pi_B \theta_{PBL}/c_p$ (see Fig. 7).

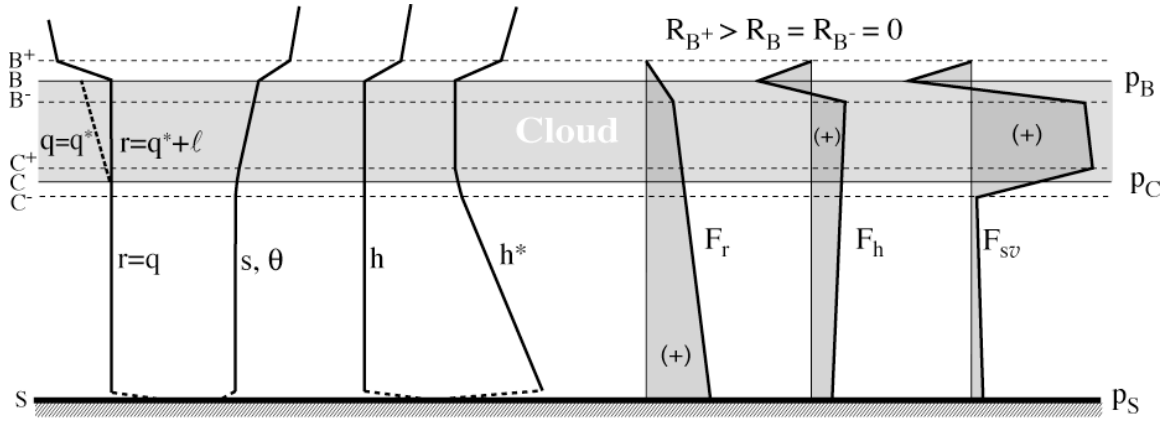

Fig. 8. Typical vertical profiles of r, q, θ, s, h , h*, F_r, F_h and F_{sv} for cloud-topped PBL.

In this case, θ and s are conserved and, therefore, vertically uniform only in the sub-cloud layer. Within the cloud layer, θ and s generally increase with height (see Fig.

8) while r and h remain uniform throughout the PBL. F_{sv} is usually negative in the subcloud layer if the surface is colder than the PBL. It is generally positive in the cloud layer, however, due to turbulence generated by radiative cooling near the top of the cloud. We can define the fluxes as follows:

Within the cloud layer ($p<p_C$):

$$F_{sv} \equiv F_s + \Pi\theta\left(0.608F_q - F_\ell\right), \tag{7.15}$$

Within the cloud layer, the air is saturated, in which the liquid water-mixing ratio is given by $\ell \equiv r - q^*$. We define the fluxes in the right hand side of (7.15) as

$$\left.\begin{aligned} F_s &= F_h - LF_{q^*} = \frac{1}{1+\gamma}F_h \\ F_q &= F_{q^*} = \frac{\gamma}{L(1+\gamma)}F_h \\ F_\ell &= F_r - F_{q^*} = F_r - \frac{\gamma}{L(1+\gamma)}F_h \end{aligned}\right\}. \tag{7.16}$$

and $\gamma \equiv \frac{L}{c_p}\left(\partial q^*/\partial T\right)_p$. From (7.15), (7.16) and defining $\beta \equiv \left(1+1.608\gamma\Pi\theta/L\right)/\left(1+\gamma\right)$, we can write F_{sv} at the top of the PBL as

$$\left(F_{sv}\right)_{B^-} = \beta_{B^-}\left(F_h\right)_{B^-} - \Pi_B\theta_{PBL}\left(F_r\right)_{B^-} \tag{7.17}$$

where $\beta_{B^-} \equiv \left(1+1.608\gamma_{B^-}\Pi_B\theta_{PBL}/L\right)/\left(1+\gamma_{B^-}\right)$ and

$$\left(F_r\right)_{B^-} = -E\left(\Delta r\right)_{B^-} = -E\left(q_{B^+} - r_{B^-}\right) \tag{7.18a}$$

and

$$\left(F_h\right)_{B^-} = -E\left(\Delta h\right)_B + \left(\Delta R\right)_B = -E\left(h_{B^+} - h_{B^-}\right) + \left(\Delta R\right)_B. \tag{7.18b}$$

In (7.17a) and (7.18b), r_{B^-} is defined in subsection 5c, and $h_{B^+} \equiv \Pi_B\theta_{B^+} + \Phi_B + Lq_{B^+}$ and $h_{B^-} = h^*_{B^-} \equiv \Pi_B\theta_{B^-} + \Phi_B + Lq^*_{B^-}$. We used (D.4) with $M_B = 0$ of Appendix D in writing (7.18a) and (7.18b). The expression we use for the entrainment rate E in (7.18a) will be

given later. We write F_{sv} at the bottom of the cloud level

$$\left(F_{sv}\right)_{C^+} \equiv \frac{1}{1+\gamma_C}\left(1+\frac{1.608\Pi_C\theta_{PBL}\gamma_C}{L}\right)\left(F_h\right)_C - \Pi_C\theta_{PBL}\left(F_r\right)_C, \tag{7.19}$$

where

$$\left.\begin{aligned}\left(F_h\right)_C &= \frac{\left(F_h\right)_S\left(p_C-p_B\right)+\left(F_h\right)_{B^-}\left(p_S-p_C\right)}{p_S-p_B}\\ \left(F_r\right)_C &= \frac{\left(F_r\right)_S\left(p_C-p_B\right)+\left(F_r\right)_{B^-}\left(p_S-p_C\right)}{p_S-p_B}\end{aligned}\right\}. \tag{7.20}$$

Note that F_{sv} is discontinuous across condensation level while F_h and F_r are continuous (see Fig. 6).

<u>Within the subcloud layer ($p>p_C$):</u>

$$F_{sv} \equiv F_s + 0.608\Pi\theta F_q, \tag{7.21}$$

where

$$\left.\begin{aligned}F_s &= F_h - LF_r\\ F_q &= F_r\end{aligned}\right\} \tag{7.22}$$

Using (7.21) and (7.22), F_{sv} at the condensation level and surface are

$$\left(F_{sv}\right)_{C^-} \equiv \left(F_h\right)_C + \left(0.608\Pi_C\theta_{PBL} - L\right)\left(F_r\right)_C, \tag{7.23}$$

and

$$\left(F_{sv}\right)_S = \left(F_h\right)_S + \left(0.608\,\Pi_S\,\theta_{PBL} - L\right)\left(F_r\right)_S = \Pi_S\left(F_\theta\right)_S + 0.608\,\Pi_S\,\theta_{PBL}\left(F_r\right)_S, \tag{7.24}$$

respectively. In (7.23), $\left(F_h\right)_C$ and $\left(F_r\right)_C$ are given by (7.20).

Buoyancy generation for this case can be written as

$$\begin{aligned}\mathcal{B} \approx\ & \kappa\left[\left(F_{sv}\right)_S + \left(F_{sv}\right)_{C^-}\right]\left(p_S-p_C\right)\Big/\left(p_S+p_C\right)\\ & +\kappa\left[\left(F_{sv}\right)_{C^+} + \left(F_{sv}\right)_{B^-}\right]\left(p_C-p_B\right)\Big/\left(p_C+p_B\right).\end{aligned} \tag{7.25}$$

Following Randall, Branson, Zhang, Moeng and Krasner (unpublished manuscript), we

calculate the entrainment rate for a cloud topped PBL by

$$E \approx \frac{b_1 \rho_{PBL} \sqrt{\tilde{e}_{PBL}} + \hat{b}_2 \beta g \left[\frac{(\delta z)_{PBL}}{\tilde{e}_{PBL}}\right] \frac{(\Delta R)_B}{\Pi_B \theta_{PBL}}}{1 + b_2 g \left[\frac{(\delta z)_{PBL}}{e_{PBL}}\right] \frac{\Delta s_v - \Delta s_{v_{crit}}}{\Pi_B \theta_{PBL}}} = \frac{b_1 \rho_{PBL} \Pi_B \theta_{PBL} \tilde{e}_{PBL}^{3/2} + \hat{b}_2 \beta_B g (\delta z)_{PBL} (\Delta R)_B}{\Pi_B \theta_{PBL} \tilde{e}_{PBL} + b_2 g (\delta z)_{PBL} \left[\Delta s_v - \Delta s_{v_{crit}}\right]}, \tag{7.26}$$

where b_1 is a constant and, $\hat{b}_2$ is defined by $b_2\left(1 - e^{-\lambda \tilde{e}_{PBL}}\right)$ with two constants b_2 and λ. In the model, b_2 is multiplied by $\left(1 - e^{-\lambda \tilde{e}_{PBL}}\right)$, where λ is arbitrarily chosen as $0.1/e_{min}$ to guarantee that $E \to 0$ as $\tilde{e}_{PBL} \to 0$. The constants b_1 and b_2 must be chosen to satisfy $b_1/b_2 = 2kC/(1-k)$ and currently $b_1 \approx 0.4$ and $b_2 \approx 0.8$ are chosen. The effect of cloud-top entrainment instability is included in (7.26) through the term with $\Delta s_v - \Delta s_{v_{crit}}$, where $(\Delta s_v)_{crit} \equiv \left[\frac{L - 1.608 \Pi_B \theta_{B^+}}{(1 + \gamma_{B^+})}\right] \times \left[q^*\left(\Pi_B \theta_{B^+}/c_p, p_B\right) - q_{B^+}\right]$. Finally we assume $(\Delta R)_B \approx (R_{LW})_{B^+}$, where R_{LW} is the longwave radiation flux. The entrainment formulation given by (7.26) is one of the formulas discussed in Stevens' (2002) comparison paper.

Determination of the shear generation in the discrete system:

We define the shear generation (7.5) in the discrete system as

$$S \approx \alpha_s \left\{ \left|(\mathbf{F_v})_S\right| \cdot \left|\mathbf{v}_M\right| + \tfrac{1}{2} E \left|\Delta \mathbf{v}\right|_B^2 \right\}, \tag{7.27}$$

where M denotes the lowest layer of PBL. In (7.27), we introduce a weighting factor α_S, which we will discuss below.

In our parameterization, we use the factor α, which depends on the Monin-Obukov length L, to scale the shear generation that can be included in the bulk parameterization. To determine L, we define a bulk Richardson number valid for the surface layer as $(R_i)_S \equiv g(\Delta\theta_v)_S (\delta z)_S / (\tilde{\theta}_v)_S |\Delta \mathbf{v}|_S^2$, where $|\Delta \mathbf{v}|_S$ is vertical wind shear near the surface, and its discrete form as

$$\left(R_i\right)_M \equiv \frac{g\left[\left(\tilde{\theta}_v\right)_S - \left(\theta_v\right)_M\right]\left(z_M - z_S\right)}{\left(\theta_v\right)_M |\mathbf{v}|_M^2}, \tag{7.28}$$

where

$$\left(\tilde{\theta}_v\right)_S \equiv \frac{c_p\left(\tilde{T}_v\right)_S}{\Pi_S} \approx \frac{c_p\, T_G\left[1 + 0.608\left(RH\right)_S q^*\left(T_G, p_S\right)\right]}{\Pi_S}, \tag{7.29}$$

where T_G is the ground temperature and $\left(RH\right)_S$ is the relative humidity near the surface approximately given by $\left(RH\right)_S \approx \left(RH\right)_{M+1/2} \equiv q_{M+1/2}/q^*\left(T_S, p_S\right)$, where $q_{M+1/2} \equiv r_M$ for $r_M < q^*\left(T_S, p_S\right)$ and $q_{M+1/2} \equiv q^*\left(T_S, p_S\right)$ for $r_M \geq q^*\left(T_S, p_S\right)$. Then we introduce the variable $\tilde{\xi}_M$, which is defined by $\left(z_M - z_S\right)/L$, where $z_M - z_S$ is the height of lowest half-layer over the surface. We can empirically write that

$$\left.\begin{array}{ll} \text{For a stable boundary layer} & \dfrac{\tilde{\xi}_M\left(0.74 + 4.7\tilde{\xi}_M\right)}{\left(1 + 4.7\tilde{\xi}_M\right)^2} = \left(R_i\right)_M > 0 \\ \text{For a neutral boundary layer} & \tilde{\xi}_M = 0 \\ \text{For an unstable boundary layer} & \tilde{\xi}_M = \left(R_i\right)_M < 0 \end{array}\right\}. \tag{7.30}$$

From (7.30), we calculate $\tilde{\xi}_M$ and then $L = \left(z_M - z_S\right)/\tilde{\xi}_M$. Finally, we calculate factor α_S from

$$\alpha_S \equiv \left[\frac{|L|}{|L| + \varepsilon\left(z_B - z_S\right)}\right]^3 \tag{7.31}$$

We currently use $\varepsilon = 10$. With (7.31), the shear contribution is virtually eliminated to the TKE generation in the parameterization when $|L|$ is very small compared to $z_B - z_S$. For this case, we assume that the shear generation is highly concentrated near the surface and it is locally balanced with the enhanced dissipation near the surface.

Determination of the PBL precipitation when $p_C > p_S$:

When $p_C > p_S$, where p_C is defined by (7.14), the precipitation takes place from the PBL to restore $p_C = p_S$. From (8.14), we can write

$$\delta p_C = \frac{p_S - p_B}{r_{PBL} - q^*_{B0}} \left[(1 + \gamma_C) \delta r_{PBL} - \frac{\gamma_C}{L} \delta h_{PBL} \right], \tag{7.32}$$

where $\delta p_C = p_C - p_S$. In (7.26), $\delta r_{PBL} = r_{PBL} - q^*_C$ and $\delta h_{PBL} \approx L \delta r_{PBL} + \Pi_{PBL} \delta \theta_{PBL}$ since $r_{PBL} = q^*_C$ and $p_C \approx p_S$ (see fig. 7). We currently assume that no condensation heating is released during this process, i.e. $\delta \theta_{PBL} = \delta h_{PBL} = 0$. From these and (7.32), we can obtain δr_{PBL} and calculate the amount of rain water from

$$P = -\delta r_{PBL} \rho_{PBL} (\delta z)_{PBL} (\delta t). \tag{7.33}$$

where (δt) is the time interval used in the integration. The loss of liquid water at each layer to the precipitation $\mathcal{R}_m$ is determined by

$$\mathcal{R}_m = \frac{\ell_m \delta r_{PBL}}{\sum_{m=L+1}^{M} \ell_m}. \tag{7.34}$$

Unstable PBL top (dry case):

If $\theta_{PBL} > \theta_{B^+}$, the PBL mixes with the layer above in the form of entrainment E. In this formulation, it is assumed that the potential temperature is a linear function of Π in the layer above PBL (see Fig. 9).

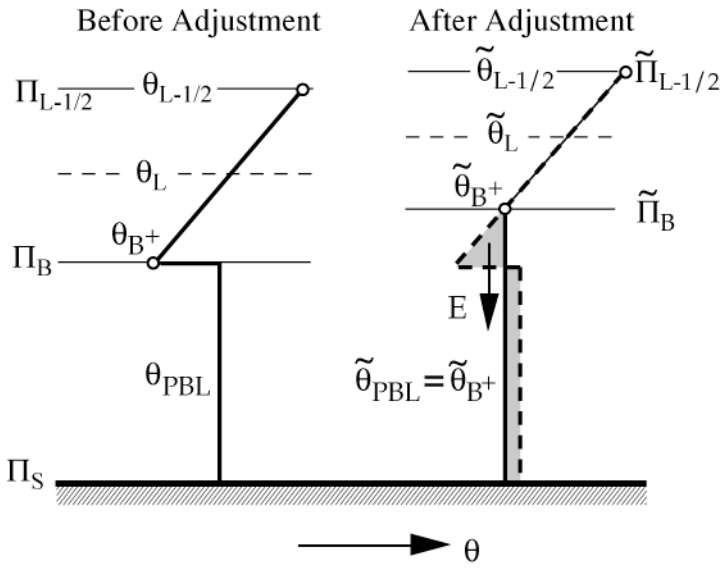

Fig. 9. Typical vertical profile of θ during the dry-convective adjustment.

The required entrainment rate E to eliminate the instability is

$$E = \frac{p_B - \tilde{p}_B}{g\delta t}. \tag{7.35}$$

where $\tilde{p}_B$ is determined from $\tilde{\Pi}_B \equiv \Pi_B - \left(\Pi_B - \Pi_{L-1/2}\right) \times \left(\tilde{\theta}_{PBL} - \theta_{B^+}\right) \Big/ \left(\theta_{L-1/2} - \theta_{B^+}\right)$ and δt is the time interval used in the integration. The final mixed layer potential temperature is give by

$$\tilde{\theta}_{PBL} \equiv \frac{\left(p_S - p_B\right)\theta_M - \frac{1}{2}\left(p_B - \tilde{p}_B\right)\theta_{B^+}}{p_S - \tilde{p}_B + \frac{1}{2}\left(p_B - \tilde{p}_B\right)}. \tag{7.36}$$

It is assumed that potential energy, which is released during the adjustment, will be converted to turbulence kinetic energy following

$$\delta e_{PBL} \equiv \frac{\left(PE\right)_{PBL} + \left(PE\right)_{B^+} - \left(\tilde{PE}\right)_{PBL}}{p_S - \tilde{p}_B}, \tag{7.37}$$

where $\left(PE\right)_{PBL}$ and $\left(\tilde{PE}\right)_{PBL}$ are the potential energy of the PBL before and after adjustment, and $\left(PE\right)_{B^+}$ is the potential energy of the air to be entrained into the PBL

during the adjustment. $(PE)_{PBL}$ and $(PE)_{B^+}$ are given by

$$(PE)_{PBL} \equiv \frac{c_p \theta_{PBL}}{g p_o^\kappa}\left[\frac{1}{\kappa+1}\left(p_B^{\kappa+1} - p_S^{\kappa+1}\right) - \left(p_S^\kappa p_B - p_S^\kappa p_S\right)\right] \tag{7.38}$$

and

$$(PE)_{B^+} \equiv \frac{c_p\left(\theta_{B^+} + \tilde{\theta}_{PBL}\right)}{2g p_o^\kappa}\left[\frac{1}{\kappa+1}\left(\tilde{p}_B^{\kappa+1} - p_B^{\kappa+1}\right) - \left(p_B^\kappa \tilde{p}_B - p_B^\kappa p_B\right)\right] + z_B\left(p_B - \tilde{p}_B\right), \tag{7.39}$$

respectively. Equation (7.39) uses an approximation for the lower portion of the layer L to be entrained, for which $\theta = \left(\theta_{B^+} + \tilde{\theta}_{PBL}\right)/2$. Finally,

$$(PE)_{B^+} \equiv \frac{c_p\left(\theta_{B^+} + \tilde{\theta}_{PBL}\right)}{2g p_o^\kappa}\left[\frac{1}{\kappa+1}\left(\tilde{p}_B^{\kappa+1} - p_B^{\kappa+1}\right) - \left(p_B^\kappa \tilde{p}_B - p_B^\kappa p_B\right)\right] + z_B\left(p_B - \tilde{p}_B\right). \tag{7.40}$$

These expressions for PE are obtained from $PE \equiv g\int_{z=z_1}^{z_2} \rho z\, dz = -\int_{p=p_1}^{p_2} z\, dp$ and $z = z_1 + \theta_1\left(\Pi_1 - \Pi\right)/g$. In the model, we apply "soft" adjustments obtained by multiplying E and δe_{PBL} by $\delta t/\tau_{dca}$, where τ_{dca} is the adjustment time scale typically 1 hour.

<u>Conditionally unstable PBL top:</u>

If $h_{PBL} > h_{B^+}^*$ for $r_{B^-} > q_{B^-}^*$, for which $h_{PBL} = h_{B^-}^* = h_C^*$, a moist convective adjustment acts in the form of PBL-top entrainment E.

The required entrainment rate E to eliminate the instability is

$$E = \frac{p_B - \tilde{p}_B}{g\delta t}. \tag{7.41}$$

where $\tilde{p}_B$ is determined from $\tilde{\Pi}_B \equiv \Pi_B - \left(\Pi_B - \Pi_{L-1/2}\right) \times \left(\tilde{h}_{PBL} - h_{B^+}\right)/\left(h_{L-1/2}^* - h_{B^+}^*\right)$. The final mixed layer moist static energy is given by

$$\tilde{h}_{PBL} \equiv \frac{(p_S - p_B)h_{PBL} + \frac{1}{2}(p_B - \tilde{p}_B)\left(h_{B^+} + \tilde{h}_{B^+}\right)}{p_S - \tilde{p}_B}. \tag{7.42}$$

See Fig. 10. It is assumed that the released Convective Available Potential Energy (CAPE) during the adjustment process is converted to the TKE following

$$\delta e_{PBL} = \frac{(CAPE)_{PBL-B^+}}{p_S - \tilde{p}_B}, \tag{7.43}$$

where

$$(CAPE)_{PBL-B^+} \approx g\frac{h_{PBL} - h^*_{B^+}}{c_p(1+\gamma)\bar{T}_{PBL-B^+}}\tilde{z}_B. \tag{7.44}$$

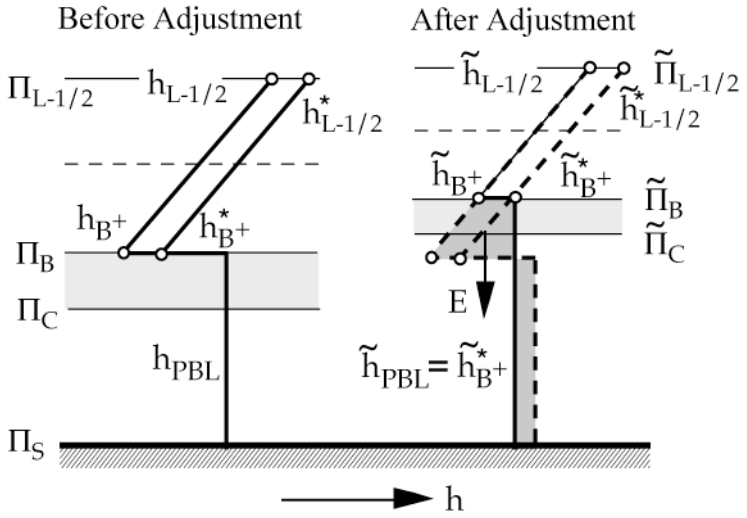

Fig. 10. Typical vertical profiles of h and h* during the moist-convective adjustment.

In the model, we apply "soft" adjustments obtained by multiplying E and δe_{PBL} by $\delta t/\tau_{mca}$, where τ_{mca} is the adjustment time scale typically 1 hour.

8. Parameterization of diffusive small-eddy effects: K-closure formulation

In our parameterization, the diffusive turbulence fluxes due to small-eddies are determined by a K-closure formulation given by (6.2). We have tested several formulations to determine the diffusion coefficient K. The earliest version of our model had a prescribed constant K_0 for the interior of the PBL and zero K's for the surface and the PBL top. Then we considered Louis' (1979) formulation for K within the subcloud layer. This is a widely used formulation to determine K locally as a function of height, grid-scale horizontal wind shear and the Richardson number. In our application, we modified Louis (1979) to fit the hybrid parameterization approach being discussed here. Here we still use a large constant $K_0 \approx 20\ \mathrm{m^2 s^{-1}}$ within the cloud layer. In our hybrid approach the grid-scale wind shear and buoyancy directly contribute to the generation of the bulk TKE, the square-root of which may be interpreted as the convective velocity scale associated with large eddies. Therefore, the diffusive eddies are generated as a result of the shear of convective velocities rather than that of grid-scale wind shear directly. To reflect this rationale, we modified Louis (1979) to use the bulk TKE divided by a length scale instead of the magnitude of grid-scale wind shear in determining the Richardson number and K. The formulation for K in our parameterization can be described as

$$K_{m+1/2} \equiv \begin{cases} \ell^2 \dfrac{\sqrt{e_{PBL}}}{(\delta z)_{PBL}} F_c(Ri) & \text{within the subcloud layer} \\ K_0 & \text{within the cloud layer} \\ 0 & \text{at the surface and PBL} - \text{top} \end{cases}, \qquad (8.1)$$

where the mixing length ℓ and the function F_C are expressed following Louis (1979). Note that $(\delta z)_{PBL}$ is used for the length scale. The Richardson number is defined by

$$Ri \equiv \frac{g\left[(\theta_e)_{m+1} - (\theta_e)_m\right](\delta z)^2_{PBL}}{(\theta_e)_{m+1/2}(\delta z)_{m+1/2}\, e_{PBL}}, \qquad (8.2)$$

which differs from the one defined by Louis (1979) in two respects. First, $e_{PBL}/(\delta z)^2_{PBL}$ is used in place of $(\partial \mathbf{v}/\partial z)^2$, the reason for which is discussed above, and, second, the potential temperature is replaced by the equivalent potential temperature. The reason for the latter is that the equivalent potential temperature is conserved under condensation process and its vertical gradient is a better measure of stability when a portion of the model layer is cloudy. We simplified the equivalent potential temperature for computational efficiency as $\theta_e \equiv \theta e^{Lq/c_p T_C}$, where we use the approximation $T_C \approx \frac{1}{2}(T_S + T_B)$. If the layer m is saturated, the saturation water vapor mixing ratio q^* is used instead of q.

9. Exchange between the PBL and free-atmosphere

In our model, the depth of PBL is a prognostic variable, the rate of which partially depends upon the PBL-top vertical mass flux determined by the entrainment parameterization. As the TKE increases due to the buoyancy and/or shear generations, the PBL tends to deepen by entraining mass from the free-atmosphere into the PBL (see Fig.11a). During the deepening, the air in the free atmosphere is not disturbed while the entrained air in the PBL is subject to vertical mixing. It is relatively straightforward to formulate this deepening process in a discrete model. The situation is very different for the collapsing PBL as shown in Fig. 11b. During the collapse, the TKE rapidly decreases and a new PBL forms from the existing surface layer. The PBL-top discontinuity tends to disappear leaving most of the well-mixed PBL air above the new shallow PBL. It requires a special consideration to formulate this process in a discrete model since the PBL top, which is a coordinate surface is rapidly displaced, which may causing computational problems such as under-shooting or over-shooting of the predicted quantities such as the water vapor mixing ratio.

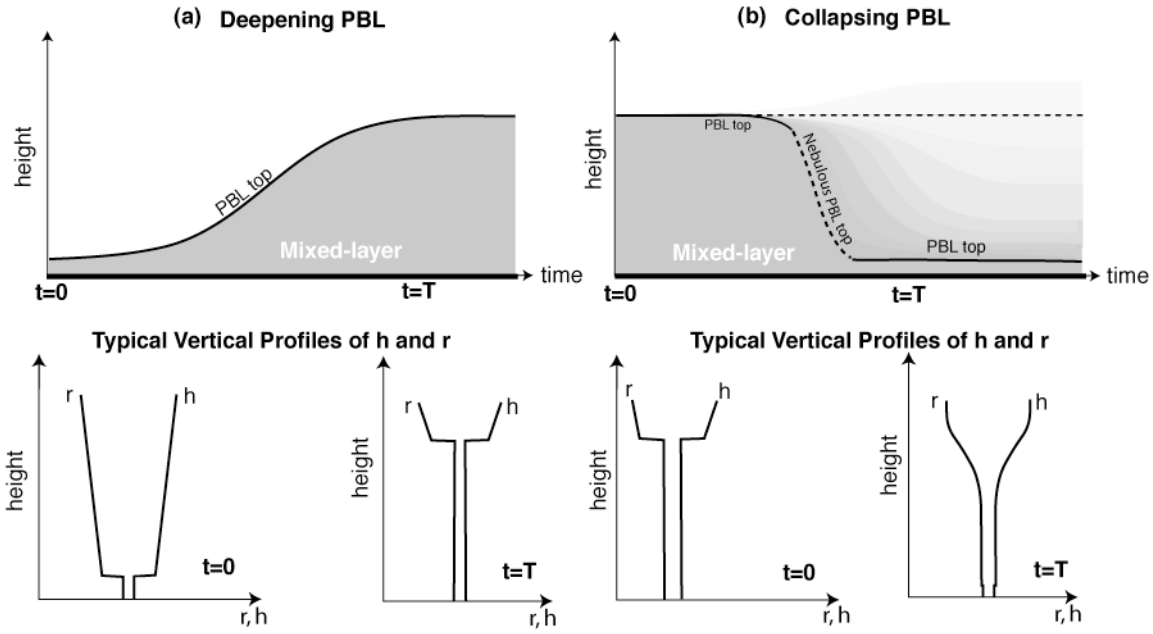

Fig. 11. Schematic illustrations of the time evolution of the PBL depth during a) deepening stage and b) collapsing stage (upper panel). The lower panel shows the typical profiles of r and h at these stages.

A realistic simulation of the exchange processes between the PBL and free-atmosphere is one of our main goals in this model. To achieve this goal, we use the specially designed formulation given in Appendix B for the discrete moisture budget equations.

10. Additional discretization aspects

a. Calculation of the condensation amount for a time-discrete case

To determine the condensation amount and condensation heating in the moisture and thermodynamic equations, respectively, we write the time discrete version of (4.3) and (4.6) with (4.4) at a fixed point in space (x,y,ζ) as

$$\left.\begin{aligned} \frac{\delta\theta}{\delta t} &= \left[1-\left(\frac{\partial\theta}{\partial\zeta}\right)A\right]\frac{LC}{\Pi} \\ \frac{\delta p}{\delta t} &= m\frac{LC}{\Pi} \\ \frac{\delta q}{\delta t} &= -\left[1+\left(\frac{\partial q}{\partial\zeta}\right)\frac{AL}{\Pi}\right]C \end{aligned}\right\}, \tag{10.1}$$

where we have used (3.5) and A is given by (4.5). In (10.1), δ operator denotes an increment for a finite time interval and $\left(\partial/\partial\zeta\right)$ represents a vertical derivative. Assuming that the initial state is supersaturated so that $q > q^*\left(\theta,p\right)$ and requiring that condensation and associated heating processes terminate at a saturated state given by $q_{final} = q^*\left(\theta+\delta\theta, p+\delta p\right)$, where q_{final} is the water vapor mixing ratio modified by condensation, we find that $\delta q \equiv q_{final} - q \approx q^*\left(\theta,p\right) + \left(\partial q^*/\partial\theta\right)_p \delta\theta + \left(\partial q^*/\partial p\right)_\theta \delta p - q$ is satisfied with (10.1) when

$$C\delta t = \frac{q-q^*}{1+\left(\frac{\partial q^*}{\partial\theta}\right)_p \frac{L}{\Pi} + A\times B}, \tag{10.2}$$

where

$$B \equiv \left(\frac{\partial q^*}{\partial p}\right)_\theta \frac{mL}{\Pi} - \left(\frac{\partial q^*}{\partial\theta}\right)_p \left(\frac{\partial\theta}{\partial\zeta}\right)\frac{L}{\Pi} + \left(\frac{\partial q}{\partial\zeta}\right)\frac{L}{\Pi}. \tag{10.3}$$

In the model, we apply "soft" adjustments due to condensation by obtaining the condensation rate C used in (5.5) and (5.6b) from $C \equiv C\delta t/\tau_{lsc}$, where τ_{lsc} is the (large-scale) condensation time scale. We currently use 30 minutes for τ_{lsc}.

We also assume that the PBL condensation process do not modify the potential temperature of the cloud free air, which is the bulk potential temperature of the PBL air.

b. Time discretization of the eddy flux terms for the PBL sub-layers

The convective eddy flux terms are integrated in time with an explicit scheme while an implicit scheme is used for the diffusive eddy terms to avoid computational instability. The procedure we use is described as follows:

$$\mathbf{v}_m^{(n+1)} = \mathbf{v}_m^{(*)} - \frac{g(\delta t)}{m^{(n+1)}}\left[\frac{\partial F_{\mathbf{v}}}{\partial \zeta}\right]_m^{(*)} - \frac{g(\delta t)}{m^{(n+1)}}\left[\frac{\partial \tilde{F}_{\mathbf{v}}}{\partial \zeta}\right]_m^{(n+1)}, \qquad (10.4a)$$

$$(m\theta)_m^{(n+1)} = (m\theta)_m^{(*)} - g(\delta t)\left\{\frac{\partial F_\theta}{\partial \zeta}\right\}_m^{(*)} - g(\delta t)\left\{\frac{\partial \tilde{F}_\theta}{\partial \zeta}\right\}_m^{(n+1)}, \qquad (10.4b)$$

$$(mr)_m^{(n+1)} = (mr)_m^{(*)} - g(\delta t)\left\{\frac{\partial F_r}{\partial \zeta}\right\}_m^{(*)} - g(\delta t)\left\{\frac{\partial \tilde{F}_r}{\partial \zeta}\right\}_m^{(n+1)}, \qquad (10.4c)$$

where (n) refers to time level and (*) refers to a state after the advection effects are implemented. The part of the solution involving the diffusive fluxes $\tilde{F}$ requires a matrix inversion.

c. Time discretization of the vertical mass flux equation

The time discretization of the vertical mass flux equation (5.13a) is as follows:

$$(m\dot{\zeta})_{\ell+1/2} = \frac{F\left(\theta_{\ell+1/2}^{(*)}, \sigma_{\ell+1/2}^{(*)}\right) - F\left(\theta_{\ell+1/2}, \sigma_{\ell+1/2}\right)}{(\delta t)\left[\left(\frac{\partial F}{\partial \theta}\right)_\sigma\left(\frac{1}{m}\frac{\partial \theta}{\partial \zeta}\right) - \left(\frac{\partial F}{\partial \sigma}\right)_\theta\left(\frac{\partial \sigma}{\partial p}\right)\right]_{\ell+1/2}^{(n+1)}} \quad \text{for } \ell = 1,2,...,L-1, \qquad (10.5a)$$

where

$$F\left(\theta_{\ell+1/2}^{(*)}, \sigma_{\ell+1/2}^{(*)}\right) - F\left(\theta_{\ell+1/2}, \sigma_{\ell+1/2}\right) \equiv \left[\left(\frac{\partial F}{\partial \theta}\right)_\sigma\right]_{\ell+1/2}^{(n)}\left[(Q/\Pi) - (\mathbf{v}\cdot\nabla\theta)\right]_{\ell+1/2}^{(n)}(\delta t)$$

$$+\left\{\left[\left(\frac{\partial F}{\partial \sigma}\right)_\theta\left(\frac{\partial \sigma}{\partial p}\right)_{p_B}\right]_{\ell+1/2}\sum_{k=1}^{\ell}\nabla\cdot(m_k\mathbf{v}_k)(\delta\zeta)_k\right\}^{(n)}(\delta t)$$

$$+\left[\left(\frac{\partial F}{\partial \sigma}\right)_{\theta}\left(\frac{\partial \sigma}{\partial p_B}\right)_{p}\right]_{\ell+1/2}^{(n)}\left\{\left[\sum_{k=1}^{L}\nabla\cdot\left(m_k\mathbf{v}_k\right)\left(\delta\zeta\right)_k\right]^{(n)}+\left(m\dot{\zeta}\right)_B\right\}\left(\delta t\right)\quad \text{for}\quad \ell=1,2,...,L-1\,. \tag{10.5b}$$

The solution of (10.5a) requires iterations since the left hand side also involves in terms, which are calculated at time level $(n+1)$. The iteration starts with the nominator of (10.5a) evaluated at $(*)$ level and continues with reevaluating it after $\theta^{(\kappa+1)}=\theta^{(\kappa)}-\left(\delta t\right)\left[\left(\frac{1}{m}\frac{\partial\theta}{\partial\zeta}\right)\right]_{\ell+1/2}^{(\kappa)}\left(m\dot{\zeta}\right)_{\ell+1/2}$ and $p^{(\kappa+1)}=p^{(\kappa)}+\left(\delta t\right)\left(m\dot{\zeta}\right)_{\ell+1/2}$ are executed. The iteration stops when $\left(m\dot{\zeta}\right)_{\ell+1/2}$ is sufficiently small and the resulting vertical mass flux can be calculated from $\left(m\dot{\zeta}\right)_{\ell+1/2}=\left(p^{(\kappa+1)}-p^{(*)}\right)\big/\delta t$.

d. Other discretization aspects

The horizontal, vertical and time discretizations used in this model closely follow Konor and Arakawa (1997), particularly those for the free-atmosphere. Here we limit our discussion on the horizontal and time discretizations used for the moisture prediction equation applied to the free-atmosphere and the PBL, and the thermodynamics equation applied to the PBL. The procedure used in the moisture equation is identical to that in the mass continuity equation, which follows Hsu and Arakawa (1990), except that it is applied to mq. In this way, we maintain the consistency between the predictions of mass and moisture in the horizontally and temporally discrete system. The procedure is based on a predictor-corrector sequence in the time integration split to the zonal and meridional directions to guarantee positive definiteness and stability.

In the thermodynamic equation applied to the PBL layers, we use Takacs' (1985) scheme except that the prognostic variable is $m\theta$. Note that Hsu and Arakawa's (1990) scheme is the positive-definite version of the Takacs' (1985) scheme.

In the PBL, the horizontal and time discretizations of the thermodynamic and moisture equations are identical to each other, both of which are based on that of the mass continuity equation except the scheme is applied to $m\theta$ and mq, respectively.

11. A numerical simulation of extratropical cyclone evolution

We have incorporated this new PBL parameterization with multiple layers in our hybrid $\theta - \sigma$ coordinate model. As mention earlier, a major advantage due to the use of multiple layers is expected to be in the simulation of PBL processes during surface frontogenesis. The multi-layer formulation allows vertical wind shears to develop and be maintained within the PBL due to a vertically varying pressure gradient force while the moist static energy is nearly well mixed in the vertical. In this way, we may expect more realistic simulations of extratropical cyclones and better predictions of low-level cloud distribution in the middle latitudes with this parameterization.

To illustrate this, we show selected results from simulations of extratropical cyclone development performed with a model that includes a multi-layer variable depth PBL parameterization and incorporates moisture and grid-scale condensation following Konor and Arakawa (2000). At this stage, the model mimics radiation processes with a simple Newtonian type heating/cooling formulation and prescribes diurnally changing (but zonally uniform) shortwave flux at the surface (see Figure 12). The model domain used in the simulations is a 9000 km by 7000 km channel on a β-plane centered at 45 deg N. The horizontal grid distance is 100 km and, there are 29 layers in the vertical, four of which are in the PBL. The model's lower boundary corresponds to the land surface, for which the ground temperature is predicted using a simple ground thermodynamics model. The zonally uniform component of the initial conditions consists of a symmetric single jet centered at the middle of the channel with 50 ms^{-1} near 300 mb. The initial relative humidity is 80% within the PBL and 75% above the PBL decreasing vertically. The simulation starts from zonally uniform fields with random perturbations.

Figure 13 displays surface pressure, "surface" potential temperature (left panel) and precipitation over the previous 6-hour period (right panel) for days 6, 8 and 10. Here the "surface" potential temperature is equal to the vertically mass-weighted average of the potential temperature for the cloud-free part of the PBL. The left panel of Fig. 13

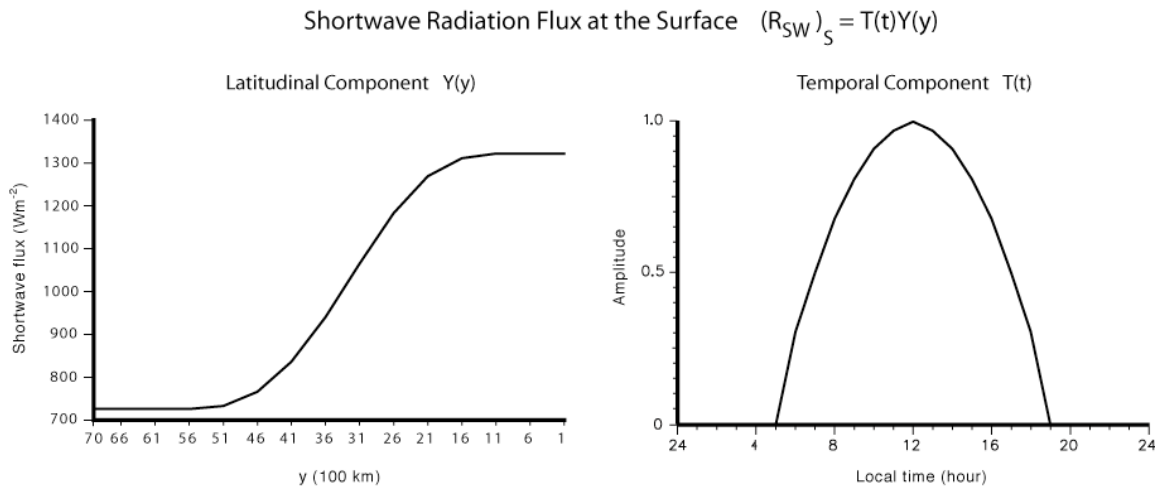

Fig. 12. Latitudinal (left) and temporal (right) components of the prescribed shortwave radiation at the surface.

shows a realistic development of extratropical cyclones and associated surface frontogenesis. The 6-hourly precipitation shown in the right panel, which results from grid-scale condensation, demonstrates a realistic amplitude and spatial pattern expected in association with developing extratropical cyclones.

To gain insight in the three-dimensional structure of the simulated flow, we present North-South cross-sections of the potential vorticity and cloudy areas (Relative Humidity≥100%) for Day 10 at hour 1200 in Fig. 14. At this stage of the simulation, the potential vorticity field indicates an intrusion of the stratospheric air into the troposphere with folding tropopause at the warm edge of the upper-level frontal zone. Clouds form and precipitation takes place as a result of the lifting and moisture convergence along cold and bent-back warm fronts. Within the PBL, clouds also form independent from the tropospheric clouds. Formation of this type of clouds will be discussed below.

To narrow down on the performance of the PBL parameterization, we present a composite diurnal change of the PBL depth and the turbulent fluxes of the moist static energy $\left(F_h\right)$ and the total water-mixing ratio $\left(F_r\right)$ within the PBL in Fig. 15. The moist static energy is defined by $h \equiv c_p T + \Phi + Lq$, where c_p is the specific heat at constant pressure, T is temperature, Φ is geopotential, L is latent heat of condensation, and q is water vapor mixing ratio. The total water mixing ratio is given by $r \equiv q$ for $r \le q^*$, where q^* is the saturation mixing ratio, and $r \equiv q^* + \ell$, where ℓ is the liquid water

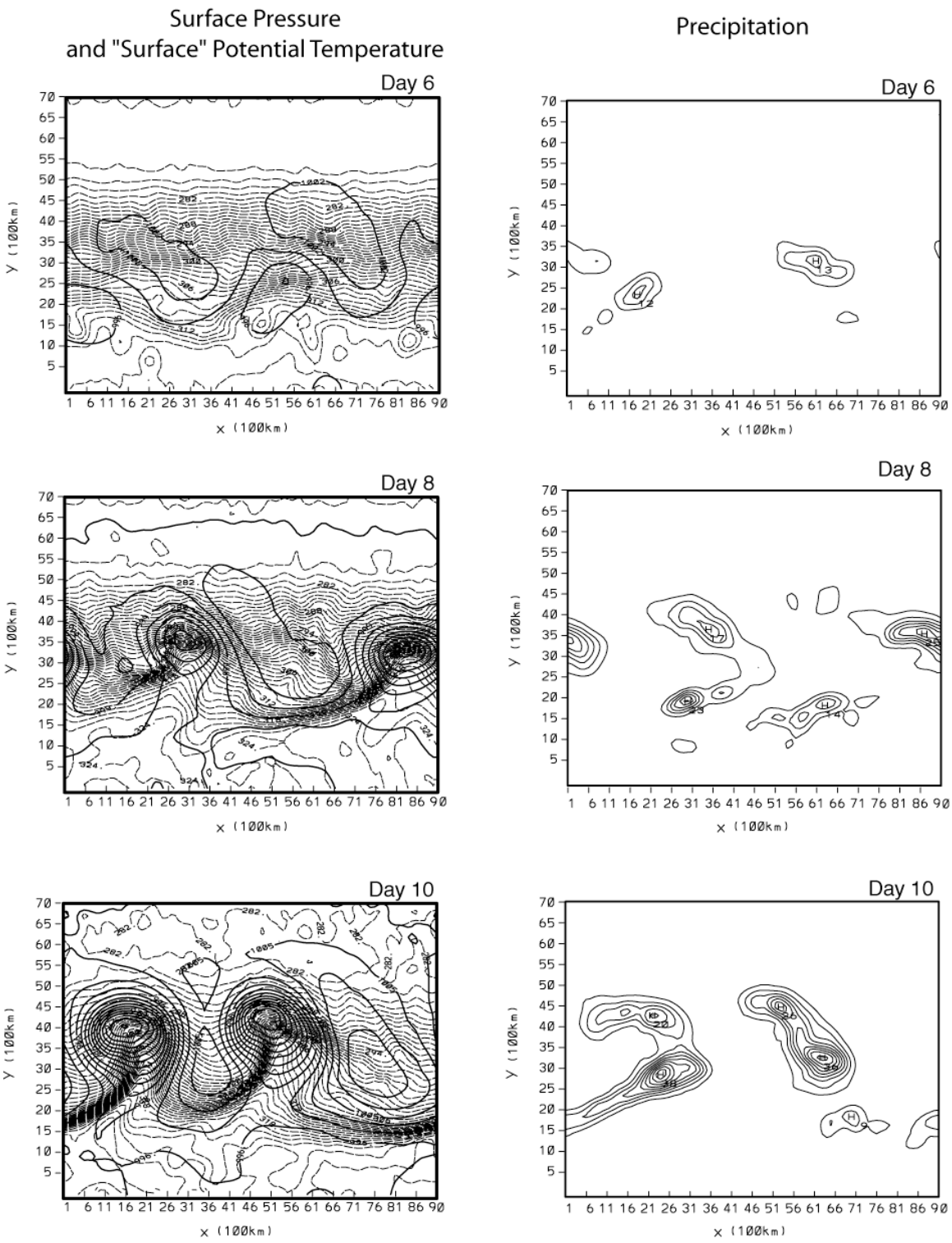

Fig. 13. Left panels show surface pressure (mb, solid lines) and “surface” potential temperature (K, dashed lines) with contour intervals 3 mb and 1K. Right panels show the precipitation (mm) during the preceding 6 hours. Smallest contour value and contour interval are 3 mm and 4 mm, respectively.

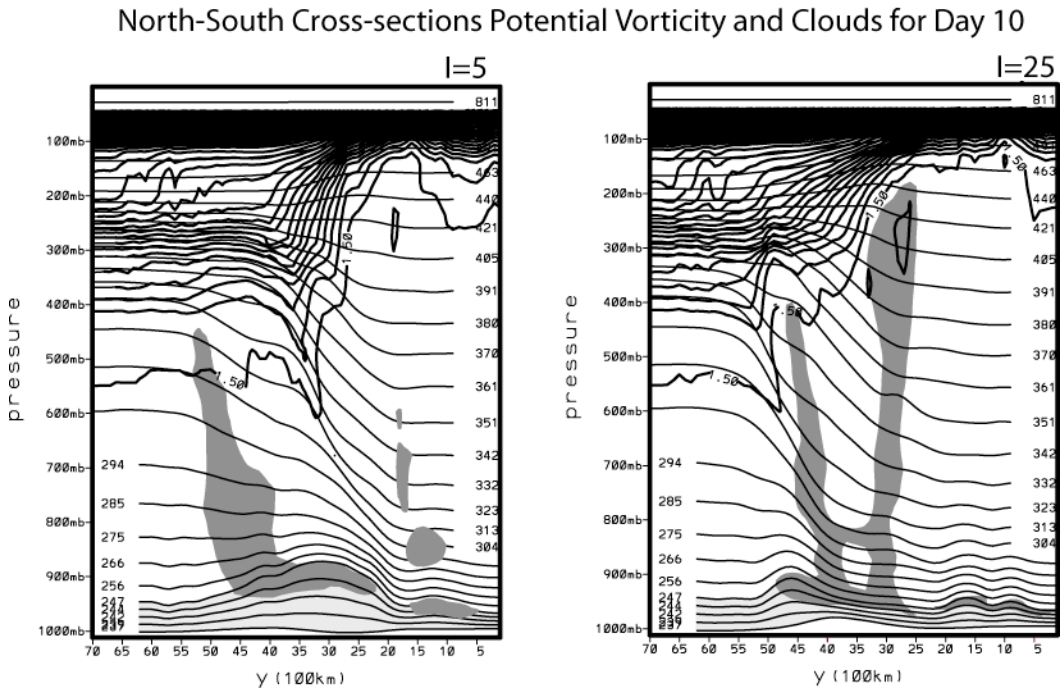

Fig. 14. Cross-sections of potential vorticity (PVU, thick lines) for Day 10 at hour 1200. Heavily shaded areas are clouds (Relative Humidity ≥100%) and the PBL is lightly shaded.

mixing ratio, and $r \equiv q^* + \ell$, where ℓ is the liquid water mixing ratio, for $r > q^*$. The PBL depth (thick solid line) in both panels of Fig. 15 shows a strong diurnal cycle: It gradually deepens in the morning hours due to the PBL-top entrainment, reaches its deepest state in the late afternoon and collapses suddenly after sunset. The upward surface fluxes of h and r, $(F_h)_S$ and $(F_r)_S$, respectively, increase in the morning hours as the ground becomes warmer reaching their maxima near hour 1300, and then decrease gradually until hour 2000. After that, $(F_h)_S$ becomes negative while $(F_r)_S$ vanishes. $(F_h)_S$ remains negative until sunrise, near hour 0700.

We also present a composite diurnal change of the PBL cloud incident in Fig. 16. The incident is determined as the fractional are coverage of PBL clouds in the absence of the clouds above PBL. During a diurnal cycle, the cloud incident is maximum shortly before sunrise within the shallow PBL. The incident frequency diminishes with time as the ground warms up before noon and it peeks again in the late afternoon when the PBL is very deep. The occurrence of PBL clouds within the deep PBL can be due to lack of radiation-cloud interactions and cumulus cloud parameterization in the current model.

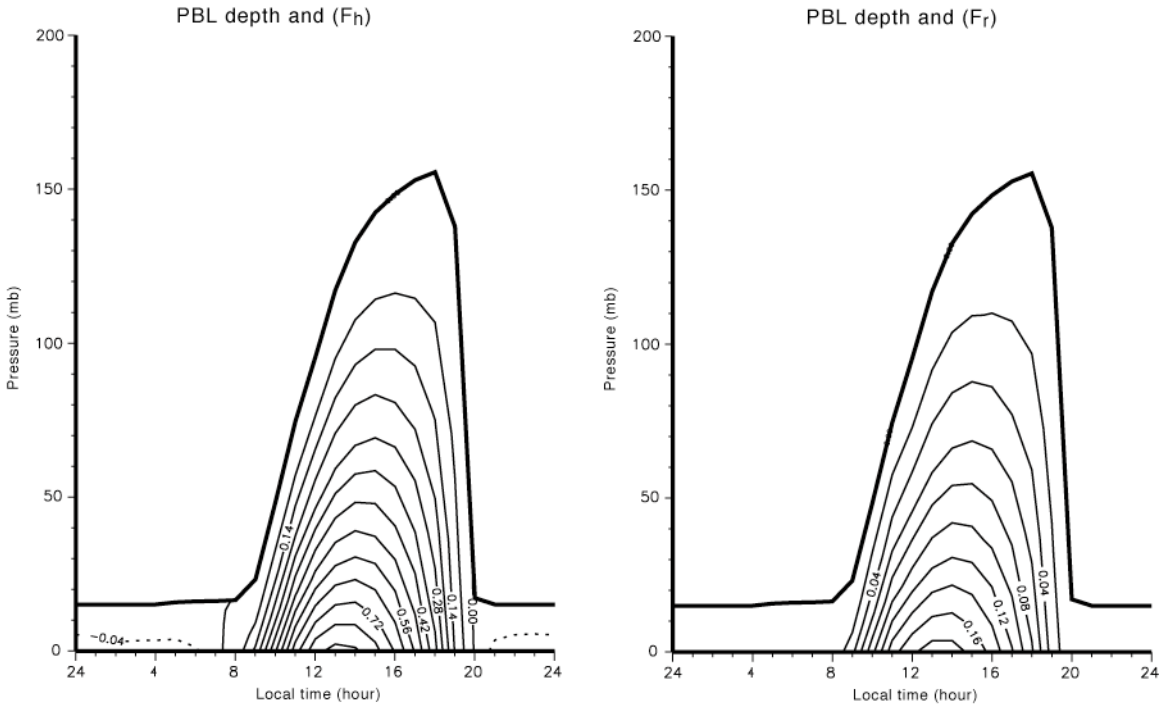

Fig. 15. Composite diurnal changes of the PBL depth (mb, thick lines), moist static energy flux F_h (10^3 Wm^{-2}, left panel, thin lines) and scaled water flux $L \times F_r$ (10^3 Wm^{-2}, right panel, thin lines).

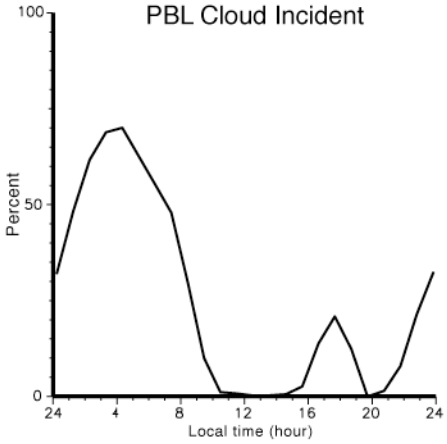

Fig. 16. Composite Composite diurnal change of PBL cloud incident.

12. Summary

In this technical report, we have presented a detailed description of the large-scale condensation process and PBL parameterization incorporated into the generalized vertical coordinate model being developed at UCLA.

The incorporation of large-scale condensation is conceptually different for an isentropic vertical coordinate model than for a pressure-based coordinate model. Konor and Arakawa (2000) present a detailed discussion on these issues and selection of a proper vertical grid to incorporate large-scale condensation processes into an isentropic model. Since the generalized vertical coordinate is an isentropic one in a large part of the vertical domain, we have closely followed Konor and Arakawa (2000) in incorporating a large-scale condensation process into the model. To avoid a vertical averaging between condensation rate and condensation heating, the prediction of moisture is placed at the interface of the model layers where the potential temperature is predicted. Konor and Arakawa's (2000) shows that an averaging can cause the dynamics to fail to take into account the change of effective static stability due to condensation.

The formulation of PBL processes remains one of the major unsolved problems in atmospheric general circulation modeling due complicated physical processes involved. A detailed simulation of the behavior and structure of the PBL would require an extremely high vertical resolution with a complex parameterization of turbulence interacting with cloud microphysics and radiation. This is usually impractical in most applications of a GCM. In this paper, we have presented a parameterization to simplify formulation of the PBL processes using a bulk approach. In this parameterization, we designate multiple variable-depth layers next to the lower boundary as the PBL. The depth of the entire PBL is predicted trough a mass budget equation including contributions of the parameterized mass entrainment (detrainment) into (out of) the PBL through the PBL top. To incorporate the variable-depth PBL into a GCM, a system of two coordinates is chosen as the vertical coordinate, one for the PBL and the other for the free atmosphere sharing the PBL top as a coordinate surface. The temperature, moisture and wind fields within the PBL are predicted using the surface fluxes and the fluxes associated with the entrainment (or detrainment) through the PBL top and diffusive fluxes between the layers. For this purpose, a hybrid parameterization is used, one of

which is the bulk parameterization and the other a K-closure formulation. The bulk parameterization is used in formulating turbulence fluxes due to convectively active large eddies, PBL-top entrainment (or detrainment), surface fluxes and PBL clouds, which is based on the predicted bulk TKE. The K-closure formulation based on a bulk Richardson number is used for the effects of diffusive small eddies cascaded from the convective large eddies. With this hybrid parameterization, simulated profiles in the PBL are allowed to deviate from well-mixed profiles, although the deviations are small for thermodynamic conservative variables when TKE is large.

We have incorporated the multi-layer PBL parameterization into our generalized vertical coordinate model using a hybrid $\theta - \sigma$ coordinate. Motivated by the encouraging results obtained by this model, the multi-layer parameterization has also been incorporated into the UCLA GCM. We will present the performance of the multi-layer PBL in climate simulations with the GCM in a forthcoming paper.

While our current multi-layer PBL parameterization significantly advances the parameterizations based on single-layer mixed-layer approach (e.g. Suarez et al., 1983), we are planning future improvements in

1) the entrainment formulation,
2) the K-closure formulation specifically designed to treat the diffusion within the subcloud layer (e.g. van Meijgaard and Ulden, 1998)
3) the prediction of the TKE for each PBL layer (e.g. Bechtold et al., 1992),
4) the parameterization of convection within the PBL by including an Arakawa-Schubert type cumulus scheme also operating in the PBL, and
5) the parameterization of horizontal structure within the PBL by including a version of the mass-flux model (e.g. Lappen and Randall, 2001a-c).

Appendix A

Vertically discrete mass and moisture continuity equations applied to the interfaces of a model based on the ζ-coordinate

Here we present vertically discrete moisture continuity equation applied to the interfaces of the model layers that is consistent with the air mass continuity equation applied to the model layers (see Arakawa and Konor, 1996). The discrete equations presented here give the corresponding mass continuity equation applied to the interfaces when a uniform distribution of q, such as $q = 1$ is assumed.

The moisture continuity equations away from the boundaries:

$$\frac{\partial (mq)_{\ell+1/2}}{\partial t} = -\nabla \cdot (qm\mathbf{v})_{\ell+1/2} - \frac{1}{(\delta\zeta)_{\ell+1/2}}\left[\left(qm\dot{\zeta}\right)_{\ell+1} - \left(qm\dot{\zeta}\right)_{\ell}\right] \text{for } \ell = 1, 2, \cdots, L-1, \quad \text{(A.1)}$$

where

$$\left.\begin{aligned} (mq)_{\ell+1/2} &\equiv q_{\ell+1/2}\left[(\delta\zeta)_{\ell+1} m_{\ell+1} + (\delta\zeta)_{\ell} m_{\ell}\right] \Big/ \left[(\delta\zeta)_{\ell+1} + (\delta\zeta)_{\ell}\right] \\ (qm\mathbf{v})_{\ell+1/2} &\equiv q_{\ell+1/2}\left[(\delta\zeta)_{\ell+1} m_{\ell+1}\mathbf{v}_{\ell+1} + (\delta\zeta)_{\ell} m_{\ell}\mathbf{v}_{\ell}\right] \Big/ \left[(\delta\zeta)_{\ell+1} + (\delta\zeta)_{\ell}\right] \\ (\delta\zeta)_{\ell+1/2} &\equiv \frac{1}{2}\left[(\delta\zeta)_{\ell+1} + (\delta\zeta)_{\ell}\right] \end{aligned}\right\}. \quad \text{(A.2)}$$

For $\left(qm\dot{\zeta}\right)_{\ell}$, we may use the following expression:

$$\left(qm\dot{\zeta}\right)_{\ell} \equiv \left[q_{\ell+1/2}\left(m\dot{\zeta}\right)_{\ell+1/2} + q_{\ell-1/2}\left(m\dot{\zeta}\right)_{\ell-1/2}\right] \Big/ 2 \qquad \text{for } \ell = 1, 2, ..., L. \quad \text{(A.4)}$$

In the model, however, an alternative definition for $\left(qm\dot{\zeta}\right)_{\ell}$ is used to obtain more accurate vertical moisture convergence in our model. See appendix B for more detail.

The moisture continuity equations at the boundaries:

At the upper boundary,

$$\frac{\partial (mq)_{1/2}}{\partial t} = -\nabla \cdot (qm\mathbf{v})_{1/2} - \frac{1}{(\delta\zeta)_{1/2}}\left(qm\dot{\zeta}\right)_{3/2}, \quad \text{(A.5)}$$

where $(\mu q)_{1/2} \equiv q_{1/2}\mu_1$, $(q\mu\mathbf{v})_{1/2} \equiv q_{1/2}\mu_1\mathbf{v}_1$ and $(\delta\zeta)_{1/2} \equiv (\delta\zeta)_1/2$. At the lower boundary,

$$\frac{\partial(\mu q)_{L+1/2}}{\partial t} = -\nabla\cdot(q\mu\mathbf{v})_{L+1/2} + \frac{1}{(\delta\zeta)_{L+1/2}}\left(q\mu\dot{\zeta}\right)_{L-1/2}, \qquad \text{(A.6)}$$

where $(\mu q)_{L+1/2} \equiv q_{L+1/2}\mu_L$, $(q\mu\mathbf{v})_{L+1/2} \equiv q_{L+1/2}\mu_L\mathbf{v}_L$ and $(\delta\zeta)_{L+1/2} \equiv (\delta\zeta)_L/2$.

When q is vertically uniform, (A.1) to (A.4) are consistent with the vertically discrete air mass continuity equation given by (5.16).

Appendix B

Vertical and temporal discretizations of the moisture budget equations

Here we present the finite-difference schemes used in the vertical moisture advection. Since our focus is on the vertical advection, we write the equations needed after the computational step of horizontal advection and three-dimensional advection of m are completed. We can vertically and temporally discretize the vertical advection of moisture as

$$(mq)_{1/2}^{(n+1)} = (mq)_{1/2}^{(*)} - (\delta t)F_1^{(*)} \Big/ (\delta\zeta)_{1/2} \quad , \tag{B.1a}$$

$$(mq)_{\ell+1/2}^{(n+1)} = (mq)_{\ell+1/2}^{(*)} - (\delta t)\left(F_{\ell+1} - F_\ell\right)^{(*)} \Big/ (\delta\zeta)_{\ell+1/2} \text{ for } \ell = 1,2,...,L-1, \tag{B.1b}$$

$$(mq)_{L+1/2}^{(n+1)} = (mq)_{L+1/2}^{(*)} - (\delta t)\left(F_{L+1/2} - F_L\right)^{(*)} \Big/ (\delta\zeta)_{L+1/2}, \tag{B.1c}$$

$$(mq)_{L+1}^{(n+1)} = (mq)_{L+1}^{(*)} - (\delta t)\left(F_{L+3/2} - F_{L+1/2}\right)^{(*)} \Big/ (\delta\zeta)_{L+1}, \tag{B.1d}$$

$$(mq)_{m}^{(n+1)} = (mq)_{m}^{(*)} - (\delta t)\left(F_{m+1/2} - F_{m-1/2}\right)^{(*)} \Big/ (\delta\zeta)_{m} \text{ for } m = L+2,...,M, \tag{B.1e}$$

where (n) refers to time level and (*) refers to a state after the horizontal advection effects are implemented at time level n.

Now we define of the fluxes in (B.1a) to (B.1e). For the free-atmosphere ($\ell = 1,2,...,L-2$), we use a positive definite scheme based on Hsu and Arakawa's (1990) third-order scheme. When $\dot{\zeta}_\ell < 0$, where $\dot{\zeta}_\ell \equiv \left[\left(m\dot{\zeta}\right)_{\ell+1/2}^{(*)} + \left(m\dot{\zeta}\right)_{\ell-1/2}^{(*)}\right] \Big/ 2m_\ell^{(n+1)}$, the flux in the scheme is defined by

$$F_\ell^{(*)} \equiv \dot{\zeta}_\ell \left[\frac{(mq)_{\ell+1/2}^{(*)} + (mq)_{\ell-1/2}^{(*)}}{2}\right]$$
$$+\dot{\zeta}_\ell \left\{-\left(\frac{1+2\gamma_\ell^-}{6}\right)\left[(mq)_{\ell+1/2}^{(*)} - (mq)_{\ell-1/2}^{(*)}\right] + \left(\frac{1-\gamma_\ell^-}{6}\right)\left[(mq)_{\ell-1/2}^{(*)} - (mq)_{\ell-3/2}^{(*)}\right]\right\}, \tag{B.2a}$$

where

$$\gamma_\ell^- \equiv \frac{\left[(mq)_{\ell-3/2}^{(*)} - 2(mq)_{\ell-1/2}^{(*)} + (mq)_{\ell+1/2}^{(*)}\right]^2}{\left[(mq)_{\ell-3/2}^{(*)} - 2(mq)_{\ell-1/2}^{(*)} + (mq)_{\ell+1/2}^{(*)}\right]^2 + (mq)_{\ell+1/2}^{(*)}(mq)_{\ell-1/2}^{(*)}}. \tag{B.2b}$$

To avoid under-shooting, we constrain the flux by

$$\left|F_{\ell}^{(*)}\right| \le \mathrm{Max}\left\{\left[m_{\ell-1/2}^{(n+1)} q_{\ell-1/2}^{\min} - (mq)_{\ell-1/2}^{(*)}\right](\delta\zeta)_{\ell-1/2} \Big/ (\delta t), 0\right\}, \qquad \text{(B.2c)}$$

where $q_{\ell-1/2}^{\min} = \mathrm{Max}\left\{q_{\ell-1/2}^{(*)}, q_{\ell-3/2}^{(*)}, q_{\ell-5/2}^{(*)}\right\}$. When $\dot{\zeta}_{\ell} > 0$, the flux is defined by

$$F_{\ell}^{(*)} \equiv \dot{\zeta}_{\ell}\left[\frac{(mq)_{\ell-1/2}^{(*)} + (mq)_{\ell+1/2}^{(*)}}{2}\right]$$
$$+\dot{\zeta}_{\ell}\left\{-\left(\frac{1+2\gamma_{\ell}^{+}}{6}\right)\left[(mq)_{\ell-1/2}^{(*)} - (mq)_{\ell+1/2}^{(*)}\right] + \left(\frac{1-\gamma_{\ell}^{+}}{6}\right)\left[(mq)_{\ell+1/2}^{(*)} - (mq)_{\ell+3/2}^{(*)}\right]\right\}, \qquad \text{(B.3a)}$$

where

$$\gamma_{\ell}^{+} \equiv \frac{\left[(mq)_{\ell-1/2}^{(*)} - 2(mq)_{\ell+1/2}^{(*)} + (mq)_{\ell+3/2}^{(*)}\right]^2}{\left[(mq)_{\ell-1/2}^{(*)} - 2(mq)_{\ell+1/2}^{(*)} + (mq)_{\ell+3/2}^{(*)}\right]^2 + (mq)_{\ell+1/2}^{(*)}(mq)_{\ell-1/2}^{(*)}}. \qquad \text{(B.3b)}$$

To avoid under-shooting, we constrain the flux by

$$\left|F_{\ell}^{(*)}\right| \le \mathrm{Max}\left\{\left[m_{\ell+1/2}^{(n+1)} q_{\ell+1/2}^{\min} - (mq)_{\ell+1/2}^{(*)}\right](\delta\zeta)_{\ell+1/2} \Big/ (\delta t), 0\right\}, \qquad \text{(B.3c)}$$

where $q_{\ell+1/2}^{\min} = \mathrm{Max}\left\{q_{\ell+3/2}^{(*)}, q_{\ell+1/2}^{(*)}, q_{\ell-1/2}^{(*)}\right\}$. Near the PBL-top, the fluxes are defined by

$$\left.\begin{aligned} F_{L}^{(*)} &\equiv q_{L-1/2}^{(*)}\left(m\dot{\zeta}\right)_{L}^{(*)} \\ F_{L+1/2}^{(*)} &\equiv q_{L+1/2}^{(*)}\left(m\dot{\zeta}\right)_{L+1/2}^{(*)} \end{aligned}\right\} \qquad \text{(B.4a)}$$

for $\left(m\dot{\zeta}\right)_{L+1/2} < 0$, and, to avoid the under-shooting, we constrain these fluxes by

$$\left|F_{L}^{(*)}\right| \le \mathrm{Max}\left\{\left[m_{L-1/2}^{(n+1)} q_{L-1/2}^{\min} - (mq)_{L-1/2}^{(*)}\right](\delta\zeta)_{L-1/2} \Big/ (\delta t), 0\right\} \qquad \text{(B.4b)}$$

with $q_{L-1/2}^{\min} \equiv \mathrm{Max}\left\{q_{L-1/2}^{(*)}, q_{L-3/2}^{(*)}, q_{L-5/2}^{(*)}\right\}$ and

$$\left|F_{L+1/2}^{(*)}\right| \le \mathrm{Max}\left\{\left[m_{L+1/2}^{(n+1)} q_{L+1/2}^{\min} - (mq)_{L+1/2}^{(*)}\right](\delta\zeta)_{L+1/2} \Big/ (\delta t), 0\right\} \qquad \text{(B.4c)}$$

with $q^{min}_{L+1/2} \equiv \mathrm{Max}\left\{q^{(*)}_{L+1/2}, q^{(*)}_{L-1/2}\right\}$. For $\left(m\dot{\xi}\right)_{L+1/2} > 0$, on the other hand, the fluxes are defined by

$$\left.\begin{aligned} F^{(*)}_{L} &\equiv r^{(*)}_{L+1/2}\left(m\dot{\xi}\right)^{(*)}_{L} \\ F^{(*)}_{L+1/2} &\equiv r^{(*)}_{L+1}\left(m\dot{\xi}\right)^{(*)}_{L+1/2} \end{aligned}\right\}. \tag{B.4d}$$

Within the PBL, the fluxes are defined by

$$\left.\begin{aligned} F^{(*)}_{m+1/2} &\equiv \frac{r^{(*)}_{m+1} + r^{(*)}_{m-1}}{2}\left(m\dot{\xi}\right)_{m+1/2} \quad \text{for } \ell = L+2,...,M-1 \\ F^{(*)}_{M+1/2} &= 0 \end{aligned}\right\}. \tag{B.5}$$

To simulate the PBL-top processes during collapse, for which $\left(m\dot{\xi}\right)_{L+1/2} > 0$ (D>0 and E=0), we constrain the values of $q^{(n+1)}_{\ell+1/2}$ in the lower free atmosphere by $q_{max} \equiv \mathrm{Max}\left\{r^{(*)}_{m} \text{ for } m = L+1, M\right\}$, which is the maximum of r within the PBL at time level (*). If $q^{(n+1)}_{\ell+1/2} > q_{max}$ for $\ell = i,...,L$ occurs, where i is obtained from $\left(p_S - p_{i+1}\right) \le \left(\delta p\right)_{max} \le \left(p_S - p_i\right)$, and thus $i+1/2$ identifies the highest interface, where q is predicted, below the properly chosen upper limit of the PBL-top given by $p_S - \left(\delta p\right)_{max}$, the excess moisture $q^{(n+1)}_{\ell+1/2} - q_{max}$ is carried upward between levels $i+1/2$ and $L+1/2$ through the procedure described below, which is referred to as "final step" in Fig. B1.

In the "final step", we first calculate

$$\left(\Delta q\right)_{\ell+1/2} \equiv q^{(n+1)}_{\ell+1/2} - q_{max} \text{ for } \ell = j,...,L, \tag{B.6a}$$

at the first step, we set j=i. Then we obtain the total available moisture to carry, $\mathcal{P}$ and the total moisture hole to fill, $\mathcal{N}$, from these definitions as follows:

$$\left.\begin{aligned} \mathcal{P} &\equiv \frac{1}{2}\sum_{\ell=1}^{L}\left[(\Delta q)_{\ell+1/2} + \left|(\Delta q)_{\ell+1/2}\right|\right] m_{\ell+1/2}^{(n+1)} \\ \mathcal{N} &\equiv \frac{1}{2}\sum_{\ell=1}^{L}\left[(\Delta q)_{\ell+1/2} - \left|(\Delta q)_{\ell+1/2}\right|\right] m_{\ell+1/2}^{(n+1)} \end{aligned}\right\}. \qquad \text{(B.6b)}$$

If $\mathcal{P} >- \mathcal{N}$, we decrease j until $-\mathcal{N} > \mathcal{P}$ is reached. Finally, we fill the moisture holes identified by $q_{\ell+1/2}^{(n+1)} < q_{max}$, without exceeding q_{max}, between j +1/2 and L +1/2 by giving priority to the lowest level and conserving mass-weighted water-vapor mixing ratio.

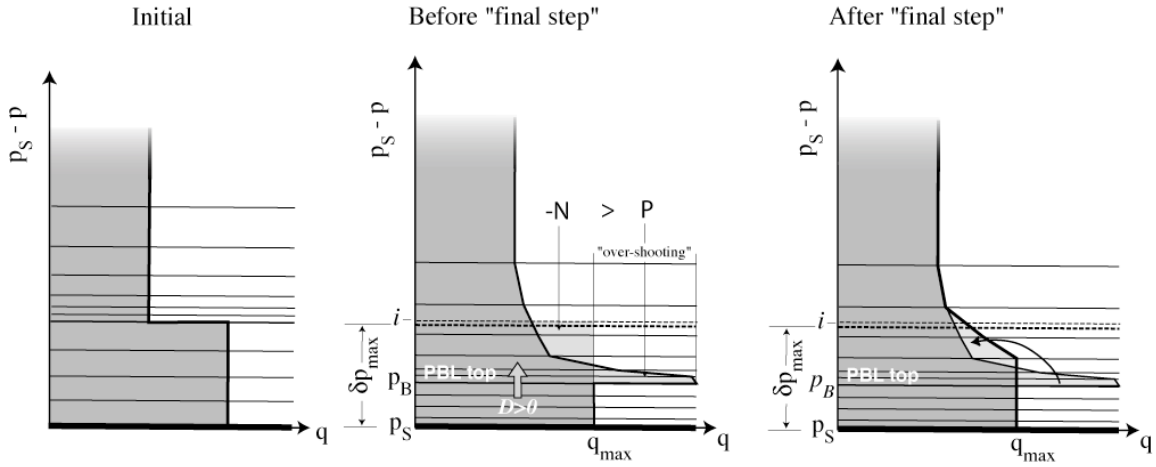

Fig. B1. Simulated vertical transport of q through the PBL-top during collapse (D>0 and E=0). Initially, q is prescribed by a step function with larger values in the PBL.

Appendix C

Pressure gradient force for the layers within the PBL

Here we present an alternative pressure gradient force term for the layers within the PBL. The derivation procedure closely follows Suarez et al. (1983) since a modified sigma coordinate is used for the PBL.

The pressure on the coordinate surfaces can be defined by

$$p = p_S - m\left(\zeta - \zeta_S\right) \text{with} \zeta_B \geq \zeta \geq \zeta_S . \tag{C.1}$$

In (C.1), the PBL mass m is defined by (6.2). Note that the subscript PBL is omitted in m_{PBL}. The pressure gradient force on the sigma surfaces is

$$-\left(\nabla\Phi\right)_p = -\nabla_\zeta\Phi + \frac{\partial\Phi}{\partial p}\nabla_\zeta p . \tag{C.2}$$

If we assume that the individual PBL layers are internally vertically well mixed, we can write the pressure gradient force (C.2) for the layer m as

$$-\left(\nabla_p\Phi\right)_m = \frac{1}{\zeta_{m+1/2} - \zeta_{m-1/2}}\int_{\zeta_{m-1/2}}^{\zeta_{m+1/2}}\left(-\nabla_\zeta\Phi\right)d\zeta + \frac{1}{\zeta_{m+1/2} - \zeta_{m-1/2}}\int_{\zeta_{m-1/2}}^{\zeta_{m+1/2}}\left(\frac{\partial\Phi}{\partial p}\nabla_\zeta p\right)d\zeta . \tag{C.3}$$

Then using (C.1) and defining

$$-\nabla\Phi_m \equiv \frac{1}{\zeta_{m+1/2} - \zeta_{m-1/2}}\int_{\zeta_{m-1/2}}^{\zeta_{m+1/2}}\left(-\nabla_\zeta\Phi\right)d\zeta \tag{C.4}$$

in (C.3), we can rewrite (C.3) as

$$-\left(\nabla_p\Phi\right)_m = -\nabla\Phi_m + \frac{1}{\zeta_{m+1/2} - \zeta_{m-1/2}}\int_{\zeta_{m-1/2}}^{\zeta_{m+1/2}}\left\{\frac{\partial\Phi}{\partial p}\nabla_\zeta\left[p_S - m\left(\zeta - \zeta_S\right)\right]\right\}d\zeta . \tag{C.5}$$

Using the hydrostatic equation given by

$$\frac{\partial\Phi}{\partial p} = -\frac{1}{m}\frac{\partial\Phi}{\partial\zeta}, \tag{C.6}$$

in (C.5), we further rewrite (C.5) as

$$-\left(\nabla_{\mathrm{p}}\Phi\right)_m = -\nabla\Phi_m - \frac{1}{\mathsf{m}\left(\zeta_{m+1/2}-\zeta_{m-1/2}\right)}\left(\nabla p_{\mathrm{S}}\right)\int_{\zeta_{m-1/2}}^{\zeta_{m+1/2}}\frac{\partial\Phi}{\partial\zeta}\mathrm{d}\zeta$$

$$+\frac{1}{\mathsf{m}\left(\sigma_{m+1/2}-\sigma_{m-1/2}\right)}\left(\nabla\mathsf{m}\right)\int_{\zeta_{m-1/2}}^{\zeta_{m+1/2}}\frac{\partial\Phi}{\partial\zeta}\zeta\mathrm{d}\zeta - \frac{1}{\mathsf{m}\left(\zeta_{m+1/2}-\zeta_{m-1/2}\right)}\zeta_{\mathrm{S}}\left(\nabla\mathsf{m}\right)\int_{\zeta_{m-1/2}}^{\zeta_{m+1/2}}\frac{\partial\Phi}{\partial\zeta}\mathrm{d}\zeta\,. \quad \text{(C.7)}$$

If we use

$$\Phi_{m+1/2}-\Phi_{m-1/2} = \int_{\zeta_{m-1/2}}^{\zeta_{m+1/2}}\frac{\partial\Phi}{\partial\zeta}\mathrm{d}\zeta\,, \quad \text{(C.8)}$$

$$\int_{\zeta_{m-1/2}}^{\zeta_{m+1/2}}\frac{\partial\Phi}{\partial\zeta}\zeta\mathrm{d}\zeta = \Phi_{m+1/2}\zeta_{m+1/2} - \Phi_{m-1/2}\zeta_{m-1/2} - \Phi_m\left(\zeta_{m+1/2}-\zeta_{m-1/2}\right) \quad \text{(C.9)}$$

and

$$\nabla p_{\mathrm{S}} = \nabla p_{\mathrm{B}} + \left(\zeta_{\mathrm{B}}-\zeta_{\mathrm{S}}\right)\nabla\mathsf{m}\,, \quad \text{(C.10)}$$

which is obtained from (C.1), we obtain the pressure gradient force for layer m of the PBL is

$$-\left(\nabla_{\mathrm{p}}\Phi\right)_m = -\nabla\Phi_m + \frac{1}{\mathsf{m}\left(\zeta_{m+1/2}-\zeta_{m-1/2}\right)}\left(\Phi_{m-1/2}-\Phi_{m+1/2}\right)\left(\nabla p_{\mathrm{B}}\right)$$
$$-\frac{\left(\nabla\mathsf{m}\right)}{\mathsf{m}\left(\zeta_{m+1/2}-\zeta_{m-1/2}\right)}\left[\zeta_{m+1/2}\left(\Phi_m-\Phi_{m+1/2}\right)+\zeta_{m-1/2}\left(\Phi_{m-1/2}-\Phi_m\right)-\zeta_{\mathrm{B}}\left(\Phi_{m-1/2}-\Phi_{m+1/2}\right)\right]. \quad \text{(C.11)}$$

Appendix D

Budget equation for ψ in the PBL

We can write the budget equation for ψ within the PBL as

$$\frac{\partial}{\partial t}\left(m\psi\right)_m + \nabla\cdot\left(\psi m\mathbf{v}\right)_m = -\frac{1}{\left(\delta\zeta\right)_m}\left[\psi_{m+1/2}\left(m\dot{\zeta}\right)_{m+1/2} - \psi_{m-1/2}\left(m\dot{\zeta}\right)_{m-1/2}\right]$$
$$-\frac{g}{\left(\delta\zeta\right)_m}\left[\left(F_\psi\right)_{m+1/2} - \left(F_\psi\right)_{m-1/2}\right] \quad \text{for } m\text{=L+2, . . ., M,} \quad \text{(D.1)}$$

where

$$\psi_{m+1/2} = f\left(\psi_m, \psi_{m+1}\right) \qquad \text{for } m\text{=L+2, . . ., M-1} \quad \text{(D.2)}$$

and F_ψ is the total turbulent flux of ψ. Note that the subscript PBL is omitted in m_{PBL}.

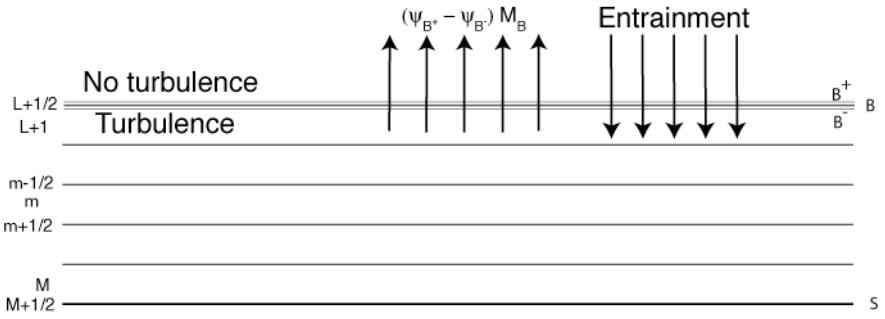

Figure D1

At the uppermost layer of the PBL, the budget equation is written following an approach similar to Suarez et al. (1983). In this approach, we assume that a thin transition layer with negligible storage separates the PBL from the free atmosphere (see Fig. D1). At the top of the transition layer (B^+), the flow is non-turbulent [i.e. $\left(F_\psi\right)_{B^+} = 0$]; and at the bottom of it (B^-), the flow is turbulent [i.e. $\left(F_\psi\right)_{B^-} \neq 0$]. For this layer, the budget equation is given by

$$\psi_{B^-}E - \psi^{(c)}_{B^-}M_B - \left(F_\psi\right)_{B^-} - \left(R_\psi\right)_{B^-} = \psi_{B^+}E - \psi^{(c)}_{B^+}M_B - \left(F_\psi\right)_{B^+} - \left(R_\psi\right)_{B^+}, \quad \text{(D.3)}$$

where c denotes the air within cumulus-induced updraft, R_ψ is the upward radiation flux of Ψ when relevant. Assuming $\psi^{(c)} = \psi^{(c)}_{B^+} = \psi_{B^-}$, requiring $\left(F_\psi\right)_{B^+} = 0$ and using (5.26) given by $\left(m\dot{\zeta}\right)_B = -g\left(E - M_B\right)$, we can write

$$-\psi_{B^-}\left(m\dot{\zeta}\right)_B - g\left(F_\psi\right)_{B^-} = -\psi_{B^+}\left(m\dot{\zeta}\right)_B + g\left(\psi_{B^+} - \psi_{B^-}\right)M_B - g\left(\Delta R_\psi\right)_B, \quad \text{(D.4)}$$

where $\left(\Delta R_\psi\right)_B \equiv \left(R_\psi\right)_{B^+} - \left(R_\psi\right)_{B^-}$. If the PBL top is a cloud top, $\left(R_\psi\right)_{B^-} \equiv \left(R_{LW}\right)_{B^-} = 0$ for $\psi \equiv \theta$, where R_{LW} is the upward longwave radiation flux. For shortwave, we assume $\left(\Delta R_{SW}\right)_B = 0$ and, therefore, $\left(\Delta R_\psi\right)_B = \left(R_{LW}\right)_{B^+}$ for $\psi \equiv \theta$. With no clouds, on the other hand, we may use $\left(\Delta R_\psi\right)_B = 0$ for $\psi \equiv \theta$. The budget equation written for the layer bounded by $L + 3/2$ and B^- is given by

$$\frac{\partial}{\partial t}\left(m\psi\right)_{L+1} + \nabla\cdot\left(\psi m\mathbf{v}\right)_{L+1} = -\frac{1}{\left(\delta\zeta\right)_{L+1}}\left[\psi_{L+3/2}\left(m\dot{\zeta}\right)_{L+3/2} - \psi_{B^-}\left(m\dot{\zeta}\right)_B\right] - \frac{g}{\left(\delta\zeta\right)_{L+1}}\left[\left(F_\psi\right)_{L+3/2} - \left(F_\psi\right)_{B^-} - \left(R_\psi\right)_{B^-}\right]. \quad \text{(D.5)}$$

Using (D.4) in (D.5), we can obtain a budget equation for the layer bounded by $L + 3/2$ and B^+ as

$$\frac{\partial}{\partial t}\left(m\psi\right)_{L+1} + \nabla\cdot\left(\psi m\mathbf{v}\right)_{L+1} = -\frac{1}{\left(\delta\zeta\right)_{L+1}}\left[\psi_{L+3/2}\left(m\dot{\zeta}\right)_{L+3/2} - \psi_{B^+}\left(m\dot{\zeta}\right)_B\right] - \frac{g}{\left(\delta\zeta\right)_{L+1}}\left[\left(F_\psi\right)_{L+3/2} + \left(\psi_{B^+} - \psi_{B^-}\right)M_B - \left(R_\psi\right)_{B^+}\right]. \quad \text{(D.6)}$$

According to the budget equations given by (D.1) and (D.6), the effect of roots of cumulus clouds is confined to the uppermost layer of the PBL. This effect may be distributed to the lower layers through adding the term $-g\lambda_m^{(c)}\left(\psi_{B^+} - \psi_{B^-}\right)M_B/\left(\delta\zeta\right)_m$ to the right hand side of (D.1), where $\lambda_m^{(c)}$ is a constant weighting coefficient

satisfying $\sum_{m=L+1}^{M} \lambda_m^{(c)} = 1$, and replacing $\left(\psi_{B^+} - \psi_{B^-}\right) M_B$ in (D.6) by $\lambda_{L+1}^{(c)} \left(\psi_{B^+} - \psi_{B^-}\right) M_B$ (see Fig. D2).

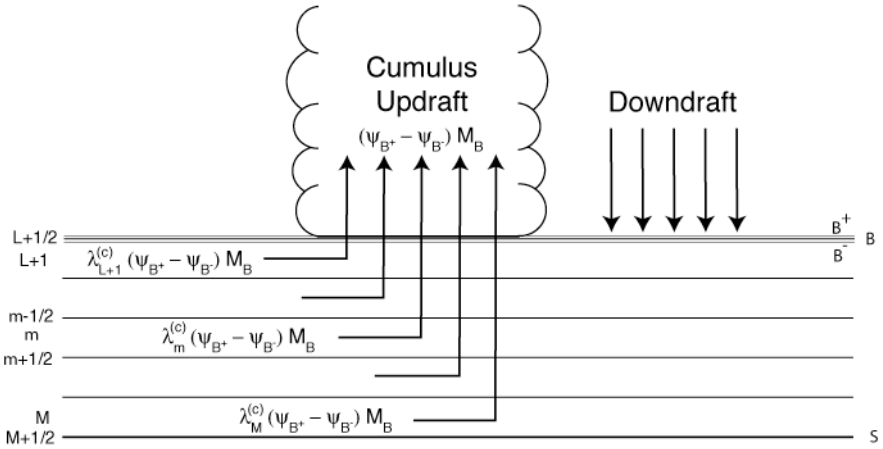

Figure D2

Appendix E

Derivation of the bulk TKE equation (7.3)

The budget equation for mass-weighted bulk TKE applied to the entire PBL can be approximately written as

$$\frac{\partial m e_{PBL}}{\partial t} = \frac{mg}{(\delta p)_{PBL}}\left(\mathcal{B} + S - \mathcal{D}\right), \tag{E.1}$$

where m is the PBL mass m_{PBL}; and $\mathcal{B}$, S and $\mathcal{D}$ are the buoyancy and shear generations and dissipation of the bulk TKE, respectively. The mass continuity equation for the PBL is

$$\frac{\partial m}{\partial t} = -\nabla\cdot(m\mathbf{v})_{PBL} + \frac{mgE}{(\delta p)_{PBL}}. \tag{E.2}$$

After multiplying (E.2) by e_{PBL} and using it in (E.1), we obtain

$$\frac{\partial e_{PBL}}{\partial t} = -\frac{e_{PBL}}{(\delta p)_{PBL}}gE + \frac{g}{(\delta p)_{PBL}}\left(\mathcal{B} + S - \mathcal{D}\right) + \frac{e_{PBL}}{m}\nabla\cdot(m\mathbf{v})_{PBL}. \tag{E.3}$$

Acknowledgments. We thank Professor David Randall for providing the bulk PBL parameterization used in this study and for his support for the ongoing research. We also thank to Mr. Gabriel Casez Boezio for his valuable help in implementing the PBL parameterization to the UCLA-GCM and performing climate simulations.

References

Arakawa, A., 1969: Parameterization of cumulus clouds. *Proceedings of the WMO/IUGG Symposium on Numerical Weather Prediction,* Tokyo, 1968, Japan Meteorological Agency, IV-8-1 to IV-8-6.

Arakawa, A, and C. S. Konor, 1996: Vertical differencing of the primitive equations based on the Charney-Phillips grid in hybrid $\sigma - p$ vertical coordinates. *Mon. Wea. Rev.,* **124**, 511-528.

Arakawa, A., 2000: A personal prospective on the early development of general circulation modeling at UCLA. In *General Circulation Model Development: Past, Present, and Future,* D. A. Randall Ed, Academic Press, 1-65.

Beljaars, A. and P. Viterbo, 1998: Role of the boundary layer in a numerical weather prediction model. *Clear and Cloudy Boundary Layers*, A. A. M. Holtslag and P. G. Duynkerke, Eds., Elsevier, 287-304.

Bechtold, P., C. Fravalo and J. P. Pinty, 1992: A model of marine boundary-layer cloudiness for mesoscale applications. *J. Atmos. Sci.,* **49**, 1723-1744.

Bleck, R., and S. Benjamin, 1993: Regional weather prediction with a model combining terrain-following and isentropic coordinates. Part I, *Mon. Wea. Rev.,* **121**, 1770-1785.

Bretherton, C. S., J. R. McCaa and H. Grenier, 2004: A New Parameterization for Shallow Cumulus Convection and Its Application to Marine Subtropical Cloud-Topped Boundary Layers. Part I: Description and 1D Results. *Mon. Wea. Rev*., **132**, 864-882.

Deardorff, J. W., 1972: Parameterization of the planetary boundary layer for use in general circulation models. *Mon. Wea. Rev.,* **100**, 93-106.

Gordon, C. T., and W. F. Stern, 1982: A description of the GFDL global spectral model. *Mon. Wea. Rev*, **110**, 625-644.

Grenier, H. and C. S. Bretherton, 2001: A moist PBL parameterization for large-scale models and its application to subtropical cloud-topped marine boundary layers. *Mon. Wea. Rev*., **129**, 357-377.

Hansen, J., G. Russell, D. Rind, P. Stone, A. Lacis, S. Lebedeff, R. Reudy, and L. Travis, 1983: Efficient three-dimensional global models for climate studies: Model I and II. *Mon. Wea. Rev*, **111**, 609-662.

Holtslag, A. A. M. and C. –H. Moeng, 1991: Eddy diffusivity and countergradient transport in the convective atmospheric boundary layer. *J. Atmos. Sci.,* **48**, 1690-1698.

Holtslag, A. A. M. and B. A. Boville, 1993: Local versus nonlocal boundary-layer diffusion in a global model. *J. Climate*, **6**, 1825-1842.

Hsu, Y-J. G., and A. Arakawa, 1990: Numerical modeling of the atmosphere with an

isentropic vertical coordinate. *Mon. Wea. Rev.,* **118**, 1933-1959.

Konor, C. S., and A. Arakawa, 1997: Design of an atmospheric model based on a generalized vertical coordinate. *Mon. Wea. Rev*., **125**, 1649-1673.

Konor, C. S., and A. Arakawa, 2000: Choice of a vertical grid in incorporating condensation heating into an isentropic coordinate model. *Mon. Wea. Rev*., **128**, 3901-3910.

Krasner, R. D., 1993: Further Development and Testing of a Second-Order Bulk Boundary Layer Model. M.S. Thesis, Department of Atmospheric Science, Colorado State University. 131 pp.

Lappen, C.-L. and D. A. Randall, 2001: Toward a unified parameterization of the boundary layer and moist convection. Part I: A new type of mass-flux model. *J. Atmos. Sci.,* **58**, 2021-2036.

Lappen, C.-L. and D. A. Randall, 2001: Toward a unified parameterization of the boundary layer and moist convection. Part III: Simulations of clear and cloudy convection. *J. Atmos. Sci.,* **58**, 2037-2051.

Lappen, C.-L. and D. A. Randall, 2001: Toward a unified parameterization of the boundary layer and moist convection. Part II: Leteral mass exchanges and subplume-scale fluxes. *J. Atmos. Sci.,* **58**, 2052-2072.

Li, J.-J. F., A. Arakawa and C. R. Mechoso, 1999: Revised planetary boundary layer moist processes in the UCLA General Circulation Model. Tenth Symposium on Global Change Studies, 10-15 January 1999, Dallas, Texas, American Meteorological Society.

Lilly, D. K., 1968: Models of cloud-topped mixed layers under a strong inversion. *Quart. J. Roy. Meteor. Soc.,* **94**, 292-309.

Lock, A. P., A. R. Brown, M. R. Bush, G. M. Martin and R. N. B. Smith, 2000: A new boundary layer scheme. PartI: Scheme description and single-column model tests. *Mon. Wea. Rev*., **128**, 3187-3199.

McCaa, J. R. and C. S. Bretherton, 2004: A New Parameterization for Shallow Cumulus Convection and Its Application to Marine Subtropical Cloud-Topped Boundary Layers. Part II: Regional Simulations of Marine Boundary Layer Clouds. *Mon. Wea. Rev*., **132**, 883-896.

Moeng, C. –H. and P. P. Sullivan, 1994: A comparison of shear- and buoyancy-driven planetary boundary layer flows. *J. Atmos. Sci.,* **51**, 999-1022.

Randall, D. A., 1976: The interaction of the planetary boundary layer with large-scale circulations. Ph.D. Thesis, Department of Atmospheric Sciences, UCLA, 247 pp.

Randall, D. A., M. A. Branson, C. Zhang, C.-H. Moeng and R. D. Krasner, 1998: An updated bulk boundary layer parameterization. *Unpublished*.

Randall, D. A., R. D. Harshvardhan, D. A. Dazlich and T. G. Corsetti, 1989: Interactions among Radiation, Convective, and Large-Scale Dynamics in a General Circulation Model, *J. Atmos. Sci*, **46**, 1943-1970.

Randall, D. A., and W. H. Schubert, 2004: Dreams of Stratocumulus sleeper. In Atmospheric Turbulence and Mesoscale Meteorology. Edited by E. Fedorovich, R. Rotunno and B. Stevens. *Cambridge University Press*. 279 pp.

Stevens, B., 2002: Entrainment in stratocumulus-topped mixed layers. *Quart. J. Roy. Meteor. Soc.*, **128**, 2663-2690.

Suarez, M. J., A. Arakawa and D .A. Randall, 1983: The parameterization of the planetary boundary layer in the UCLA general circulation model: formulation

and results. *Mon. Wea. Rev.,* **111**, 2224-2243.

Sud, Y. C. and G. K. Walker, 1992: A review of recent research on improvement of physical parameterizations in the GLA GCM. In Physical Processes in atmospheric models, D. R. Sikka and S.S. Singh (eds.), Wiley Eastern Ltd., New Delhi, 422-479.

Takacs, L. L., 1985: A two-step scheme for the advection equation with minimized dissipation and dispersion errors. *Mon. Wea. Rev.,* **113**, 1050-1065.

van Meijgaard, E. and A. P. van Ulden, 1998: A first-order mixing and condensation scheme for nocturnal stratocumulus. *Atmos. Res.,* **45**, 253-273.

Wyngaard, J. C., and C.-H. Moeng, 1990: A global survey of PBL models used within GCMs. *In proceedings of PBL model evaluation workshop: European Centre for Medium-Range Forecasts*, P. Taylor and J. C. Wyngaard (Eds.), 14-15 August, 1989, Reading, U.K., World Climate Research Program Series 42, WMO/TD 378.